

AN ABSTRACT OF THE THESIS OF

Myo Thiha Zaw for the degree of Master of Science in Civil Engineering presented on March 5, 2021

Title: Automated Chemical Acidification Testing of Cementitious Materials

Abstract approved:

W. Jason Weiss

O. Burkan Isgor

Due to its availability, versatility, structural capability, and economic advantages, concrete is the most widely used material in building sewer networks and other wastewater structures such as treatment stations, wastewater digesters, septic tanks, pumping stations, hydraulic risers, utility risers and covers, etc. Concrete structures exposed to sewer environments can experience Microbially Induced Corrosion of Concrete (MICC), which is multi-stage biological deterioration process. Three main testing procedures are typically used to assess MICC of paste, mortar, or concrete: 1) the biological chamber test that uses hydrogen sulfide (H₂S), 2) the biogenic acidification test without H₂S presence, and 3) the chemical acidification test, which is economical and straightforward to set up. These tests simulate the environment of MICC in different ways to study the corrosion process. The first part of the thesis focuses on the primary concern of the chemical acidification test, which is the rapid rising of the pH in the exposure solution due to the leaching of calcium compounds from the cementitious materials. A holistic approach was developed to stabilize the pH of the exposure solution, to measure corrosion parameters with minimal disturbance to the test, and to establish a relationship between the chemical acidification test and the theoretical systems widely used in the industry to calculate the service life of concrete.

To quantify MICC, many researchers attempt to measure mechanical properties of the concrete after exposure to the corrosive environment. Ball-on-three-ball (B3B) flexural

strength test had been recognized as the most robust test in a way that it has multiple advantages over its counterparts. The second part of this thesis addresses the questions that have surfaced with the recent adoption of this test method in ASTM C1904-20. The first question is whether the technique of mixing used in sample preparation impacts the results. It was found that the use of vacuum mixing (ASTM C1904-20) and Hobart mixing (ASTM C277, C305) provide comparable results; however, the high-shear mixing (ASTM C1738) is statistically different. The second question is how rapidly the B3B test sample needs to be tested after removal from the solution to minimize the impact of drying. It was found that the sample should be removed and tested within ten minutes to reduce variation. These results will provide information needed to evaluate changes for ASTM C1904-20.

©Copyright by Myo Thiha Zaw
March 5, 2021
All Rights Reserved

Automated Chemical Acidification Testing of Cementitious Materials

by
Myo Thiha Zaw

A THESIS

submitted to

Oregon State University

In partial fulfillment of
the requirements for the
degree of

Master of Science

Presented March 5, 2021
Commencement June 2021

Master of Science thesis of Myo Thiha Zaw presented on March 5, 2021

APPROVED:

Co-Major Professor, representing Civil Engineering

Co-Major Professor, representing Civil Engineering

Head of the School of Civil and Construction Engineering

Dean of the Graduate School

I understand that my thesis will become part of the permanent collection of Oregon State University libraries. My signature below authorizes release of my thesis to any reader upon request.

Myo Thiha Zaw, Author

ACKNOWLEDGEMENTS

I would like to express my deepest gratitude to my advisors Dr. Jason Weiss and Dr. Burkan Isgor for their support and wisdom throughout my entire program. Without their guidance, I would not be able to accomplish my research project as I did today. I am very grateful to Dr. Weiss for giving me a chance to continue my study at Oregon State University as a Master student. I firmly believe this opportunity will be the crucial foundation for success in my future career.

I would also like to express my appreciation to “Concrete Sealants, Inc.” that made this research project possible with their financial support. I am grateful to this company for providing materials that was used and tested in my study.

I would also like to thank my committee members: Dr. John Gambatese and Dr. Mariapaolo Riggio for taking their time to participate in my thesis defense.

Furthermore, I would like to thank my senior coworkers and mentors: Kai Coldsnow, Pratik Vinod Murkute, Ali Riza Erbehtas and Rita Maria Ghantous who have shared their thoughts and experiences with me to do well in my work. Their help has been vital in my effort to mitigate obstacles in my research and to improve the quality of my work.

Finally, I would like to thank my parents for their constant support throughout the entire time when I was away from home studying abroad.

CONTRIBUTION OF AUTHORS

Dr. W. Jason Weiss (advisor) and Dr. O. Burkan Isgor (co-advisor) were involved in the writing of Chapter 1, Chapter 2, and Chapter 3.

TABLE OF CONTENTS

	<u>Page</u>
1. GENERAL INTRODUCTION.....	1
1.1. Background.....	1
1.2. MICC testing.....	5
1.4. Thesis Organization.....	9
1.5. References	10
2. AUTOMATED CHEMICAL ACID IMMERSION TEST OF CEMENTITIOUS MATERIALS	18
2.1. Introduction.....	18
2.2. Materials and Methods	20
2.2.1. Overview.....	20
2.2.2. Preparation of paste specimens	21
2.2.3. Preparation of the initial exposure and titration solutions.....	22
2.2.4. Auto-titration setup and operation	24
2.2.5. Calcium ion concentration measurement	27
2.2.6. Sulfate ion concentration measurement	27
2.2.7. Acid consumption.....	28
2.2.8. Visual observation on the specimens and the exposure solutions	28
2.2.9. The ball-on-three-ball (B3B) flexural strength test	28
2.3. Results	30
2.3.1. Performance of the auto-titration setup in pH stabilization	30
2.3.2. Calcium ion concentration	31
2.3.3. Sulfate ion concentration	33
2.3.4. Acid consumption.....	35
2.3.5. Visual observation on the specimens and the exposure solutions	37
2.3.6. The B3B flexural strength test.....	40
2.4. Discussion.....	42
2.5. Conclusion	44
2.6. Acknowledgements	45
2.7. References.....	45

TABLE OF CONTENTS

	<u>Page</u>
3. DETERMINING THE INFLUENCE OF SPECIMEN MIXING PROCEDURE AND DRYING TIME ON THE RESULTS OF THE B3B FLEXURAL STRENGTH TEST	49
3.1. Background and Motivation	49
3.2. Objectives	53
3.3. Materials	54
3.4. Specimens Preparation Procedures	55
3.5. Data Acquisition Procedure	56
3.6. Data Analysis	57
3.6.1. Evaluation of the Impact of the Flexural Strength in Paste Made with Different Mixers	57
3.7. Conclusions.....	64
3.8. Acknowledgments.....	64
3.9. Reference	64
4. CONCLUSION.....	69
4.1. Conclusion from Chapter-2.....	69
4.2. Conclusion from Chapter-3.....	70
BIBLIOGRAPHY.....	72
APPENDIX - PRELIMINARY AND EXPLORATORY STUDIES TO STABILIZE THE PH IN CHEMICAL ACIDIFICATION TESTS.....	82
A.1. Background	82
A.2. Objectives	82
A.3. Materials and Methods	83
A.4. Results and Discussion	87
A.5. Conclusion	91

LIST OF FIGURES

<u>Figure</u>	<u>Page</u>
Figure-1.1: (A) and (B) show examples of deteriorated concrete manholes and (C) more severe deterioration in wastewater catchment basin.....	2
Figure-1.2: Biological process that leads to MICC of a concrete sewer pipe.....	4
Figure-1.3: Design configuration of biological growth chamber test developed by House and later used by Ding	7
Figure-1.4: Schematic diagram of benchtop biogenic immersion test set up used by Yousefi et al V/S represents the ratio of liquid volume to surface area of the cement paste specimens.....	8
Figure-2.1: Rapid rise of pH within minutes to hours after cement paste specimens were immersed in sulfuric acid solutions that were initially at pH2 and pH5.....	19
Figure-2.2: A typical cell with specimens in the initial exposure solution.....	23
Figure-2.3: Diagram of a pH Controller Setup	25
Figure-2.4: pH monitored for 24 hours during trial by using automated pH controller at initial pH level 2 and 5	27
Figure-2.5: Ball-on-three-ball test setup.	29
Figure-2.6: Average of 24-hours pH data collected by pH data logger.	31
Figure-2.7: Calcium concentration in molarity (M) measured in specimens containers (a) with four different pHs for over 1000 hours (or) 42 days, and (b) in comparison of OPC and AM.....	33
Figure-2.8: Sulfate concentrations in mg/L measured in specimen containers (a) with four different pHs for over 1000 hours or 42 days, and (b) in comparison of OPC and AM	35
Figure-2.9: a) acid consumption in the four different pH cells, b) acid consumption compared between OPC and AM specimens.....	36
Figure-2.10: The precipitation in white color around the specimens in pH2 sulfuric acid solution after 14 days	37
Figure-2.11: The appearance of specimens are compared before (left) and after (right) immersion of 21 days. The specimen in pH1 solution encountered the most severe corrosion while the specimen in pH4 solution remained visually undamaged.....	38
Figure-2.12: The appearance of specimens are compared before (left) and after (right) immersion of 42 days. The specimen from pH2 solution encountered the most severe corrosion (similar to pH1 at 21 days) while the specimen from pH3 and pH4 solution remained visually undamaged. The specimen in pH1 solution was completely deteriorated.....	39
Figure-2.13: Specimens in pH1 solution were completely failed at around 27 days.....	39

LIST OF FIGURES (CONTINUED)

<u>Figure</u>	<u>Page</u>
Figure-2.14: The AM specimens were compared against the OPC specimens after 42 days of immersion in pH2 and pH3 solutions	40
Figure-2.15: average retained flexural strength in percent (%) over 42 days of immersion: the specimens in pH1 cells were completely deteriorated around day 27 before the second test	42
Figure-2.16: the retained flexural strength (%) of AM specimens compared against OPC in pH2 and pH3 solutions	42
Figure-2.17: The rate of change of thickness, mm loss per year in terms of pH	43
Figure-3.1: Ball-on-Three-Ball (B3B) Test Setup	50
Figure-3.2: Simplifications for the Calculation of Flexural Strength in the B3B test: a) $f(\alpha, \beta, v)/t^2$ plotted as a function of thickness b) error associated with the use of equation-6.....	52
Figure-3.3: The average flexural strengths of cement paste and two mortars prepared by Vacuum, Hobart, and Waring blenders	58
Figure-3.4: The flexural strength of paste samples as a function of drying time	61
Figure-3.5: COV initially fluctuates below 6% and starts increasing at 25 minutes (a square root drying time of 5 square root minutes).....	61
Figure-A1: 1). Close glass, 2). Open glass, 3). Open plastic, and 4). Close plastic containers of sulfuric acid solution without any samples	85
Figure-A2: Three types of solutions in Test-3: a) sulfuric acid solution, b) acetic acid solution with sulfuric acid, and c) acetate buffer solution with sulfuric acid	86
Figure-A3: pH5 rose significantly in the first 30 minutes in both ratios while pH2 only slightly increased in the larger amount of solution	87
Figure-A4: pH2 solution had capacity to prevent external pH stimulations	88
Figure-A5: pH5 solution encountered external pH stimulations. Atmosphere and plastic container relatively affected the change of pH	89
Figure-A6: even acetate buffer solution in pH2 encountered the rise of pH due to one cement paste specimen	90
Figure-A7: rapid rise of pH occurred in sulfuric acid solution and gradual rise of pH in buffer solutions.....	92

LIST OF TABLES

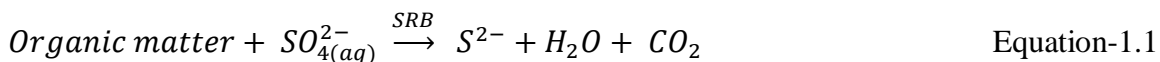
<u>Table</u>	<u>Page</u>
Table-2.1: Oxide Composition of the Type I/II ordinary portland cement (OPC) in compliance with ASTM C150	21
Table-2.2: Summary of Mixture Designs.....	22
Table-3.1: Oxide Composition of the Type I/II ordinary portland cement (OPC) ASTM C150 and AASHTO M85.....	53
Table-3.2: Mixture proportions used in this investigation (Mass in lb).....	54
Table-3.3: Number of Thin-Disc Specimens Tested for Each Mixing Procedure and The Drying Test	55
Table-3.4: Summary of Statistics Collected from Paste and Mortars Specimens from Three Types of Mixers	58
Table-3.5: Summary of the Tukey Significance Test Result on the Influence of Different Types of Mixers	59
Table-3.6: Summary of Statistics Collected from Paste and Mortars Specimens from Hobart and Waring Blenders	59
Table-3.7: Summary of Tukey Significance Test Result on the Strength Variation between Paste and Mortars	60
Table-3.8: Summary of Statistics Collected from Paste Specimens from Vacuum Blenders	62
Table-3.9: Summary of Tukey Significance Test Result on the Influence of Drying Time	62
Table-A1: Summary of information on the preliminary and exploratory tests	85

1. GENERAL INTRODUCTION

1.1. Background

Due to its availability, versatility, structural capability, and economic advantages, concrete is the most widely used material in building sewer networks and other wastewater structures such as treatment stations, wastewater digesters, septic tanks, pumping stations, hydraulic risers, utility risers and covers, etc. In 2017, the American Society of Civil Engineers (ASCE) reported a grade of D+ for the condition of sewer infrastructure in the United States, which includes 800,000 miles of public sewer pipes and 500,000 miles of private lateral sewers ^[1]. This report indicates that sewer networks in the United States are near or over their design life due to Microbially Induced Corrosion of Concrete (commonly referred to as MIC or MICC) ^[2-6], and about a \$271 billion of investment is needed over the next 25 years to maintain a healthy wastewater infrastructure. However, MICC is a serious global problem that is prevalent both in highly developed ^[6-10] and developing parts of the world ^[4, 11-13].

Wastewater contains excess amounts of sulfur compounds ^[14, 15] and anaerobic sulfur-reducing bacteria (SRB) such as *Desulfovibrio desulfuricans* ^[2, 16]. In the anaerobic environment of wastewater, where dissolved oxygen (DO) content is low (e.g., ~0.1 mg/L)^[17], SRB can use the organic matter as electron donor and sulfate ions (SO₄²⁻) as electron receptors to produce sulfides (S²⁻), which are later converted to (dissolved) H₂S_(aq) in the presence of hydrogen, as shown in the following equations^[18]:



Over time, H₂S_(aq) converts to gaseous H₂S_(g), which is released into the headspace of wastewater line. If this headspace is closed (as in the case of sewers, pipes, manholes, etc.),

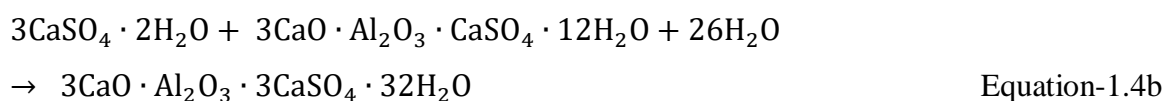
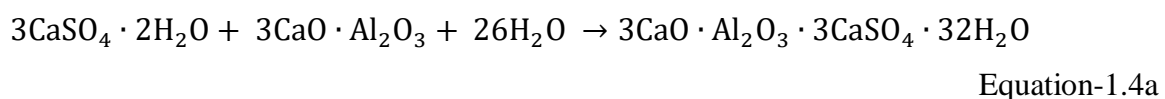
$H_2S_{(g)}$ can dissolve in the moisture layer on concrete surfaces, where sulfur-oxidizing bacteria (SOB) (e.g., *Halothiobacillus Neapolitanus* and *Acidithiobacillus Thiooxidans*)^[19-21] can oxidize it to form sulfuric acid (H_2SO_4)^[3, 22, 23]. This acid attacks the cementitious matrix of concrete, which is rich in calcium hydroxide $Ca(OH)_2$ (the main compound that gives concrete its high $pH > 12.5$)^[24-26] and calcium-silicate-hydrates (C-S-H), which provides the concrete with its strength and durability^[25, 26]. The dissociated calcium ions from CH and C-S-H react with sulfate ions from sulfuric acid to form expansive and weak products such as gypsum ($CaSO_4 \cdot 2H_2O$) and ettringite ($3CaO \cdot Al_2O_3 \cdot 3CaSO_4 \cdot 32H_2O$)^[27-29], leading to extensive deterioration of concrete, as shown in Figure-1.1.



Figure-1.1: (A) and (B) show examples of deteriorated concrete manholes and (C) more severe deterioration in wastewater catchment basins [6].

While gypsum is mostly observed in structures suffering MICC, ettringite is also reported to be found occasionally^[30, 31]. At higher pHs, the formation of ettringite follows the initial formation of gypsum. Equation-1.3 shows the initial formation of gypsum and equation-1.4a and -1.4b show ettringite formation^[32, 33]. As pH decreases due to constant biogenic acidification, ettringite becomes unstable. At this point, as described in equation 1.6, sulfuric acid attacks C-S-H, which decomposes it into silica gel and gypsum, which remain

the dominant corrosion product eventually ^[33-36]. Therefore, in the early stages of corrosion, ettringite can be found in the layer closest to the undamaged portion of concrete. As the environment becomes more acidic, ettringite becomes unstable, and gypsum starts to form as the primary corrosion product of MICC ^[33, 36].



The deterioration of concrete due to MICC is typically defined through a three-stage mechanism. Stage-1 involves the abiotic reduction of surface pH that does not involve any bacterial activity. Initially, concrete is highly alkaline with a pH usually between 12.5 and 14. However, atmospheric carbonation is one of the initial factors that slightly reduce the surface pH of the concrete ^[26]. Continuous exposure to water and/or wastewater can also further reduce the surface pH by leaching some of the ions that give concrete its high pH (e.g., Ca^{2+} , K^+ , Na^+) ^[37]. In addition, oxidation of atmospheric H_2S generates thiosulfuric and polythionic acid which potentially causes the abiotic surface pH reduction ^[38]. These processes in Stage-1 contribute to the inevitable abiotic pH reduction of concrete without bacterial involvement. When the pH decreases to about pH 9, the concrete surface become a habitat for SOB biofilm communities ^[3, 9, 11]. The overall MICC process is illustrated in Figure-1.2.

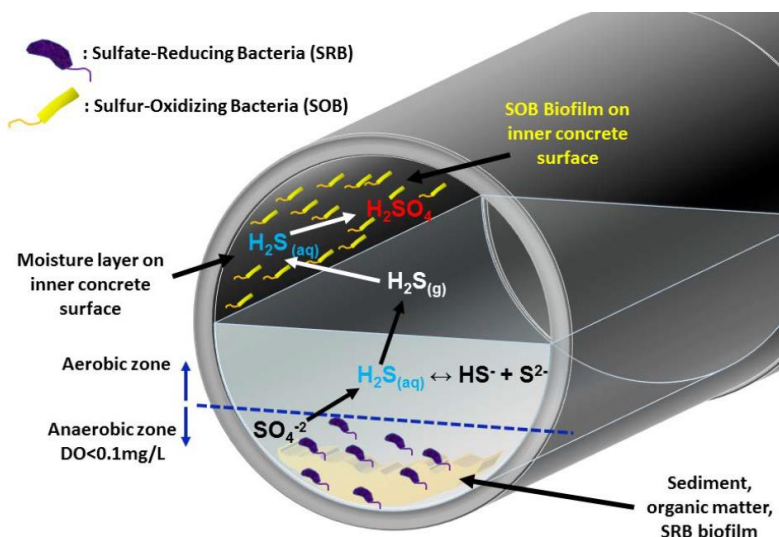


Figure-1.2: Biological process that leads to MICC of a concrete sewer pipe [39]

The Stage-2 of MICC begins when SOB bacteria can colonize on the surface of the concrete at a lower pH (~9) in the presence of sufficient nutrients, oxygen and moisture. Initial bacteria species that thrive in Stage-2 are typically Neutrophilic Sulfur-oxidizing Bacteria (NSOB) (e.g., *Thiobacillus tioparus*, *Starkeya novella*, *Halothiobacillus neopolitanus*, *Thiobacillus intermedius*), which are generally active in the pH range between 9 and 3. More information on the pH range in which each NSOB is most active can be found in the following references [3, 9, 11, 12, 16]. NSOB is responsible for mild biogenic acidification of concrete surface by consuming H_2S and other sulfur-containing compounds such as thiosulfate, polysulfate and elemental sulfur, to produce polythionic and sulfuric acids [3, 11, 16, 28, 29]. Stage-2 is assumed to be complete when pH of concrete surface reduces to approximately 4, when Acidophilic Sulfur-oxidizing Bacteria (ASOB) starts to dominate bacterial colonization [3, 11, 28, 29, 40].

The Stage-3 of MICC is when the most severe biogenic acid attack occurs. It starts when ASOB (e.g., *Acidithiobacillus ferrooxidans* and *Acidithiobacillus thiooxidans*) become the dominant microbial colonies, which are highly active in a pH range between 3-4 and 0.5 [11, 12, 41-43]. As the last and the most aggressive species of biogenic acidification cycle,

ASOB continues sulfur-oxidizing process and produces sulfuric acid at an increasing rate. As a result, surface pH drops quickly and corrosion accelerates, which significantly reduces the service life of concrete structures used in the sewer system.

1.2. MICC testing

MICC is a subject that is extensively researched in the laboratory [22, 33, 37, 44-46] and in the field [14, 29, 47, 48]. To assess the conditions of existing concrete structures exposed to wastewater and to design concrete mixtures for new structures that can resist or delay the process of MICC, many researchers have attempted to develop test methods to simulate the environment of MICC in laboratories. The testing to assess the MICC can be categorized primarily into three methods: (1) chemical acidification test, (2) biological chamber test, and (3) biogenic acidification test [22, 33, 37, 39, 45, 46]. Chemical acidification testing is based on the use of sulfuric acid to simulate the acidified environment that deteriorates concrete. Biological chamber test simulates the actual field conditions in laboratory settings where $H_2S_{(g)}$ is converted to sulfuric acid through microbial activity. Biogenic test uses bacteria that can use elemental sulfur or sulfur-containing compounds other than H_2S to create sulfuric acid.

ASTM C1898 [49] has recently been published and is recognized as the standard procedure for determining the chemical resistance of concrete products to acid attack, and provides significant improvements of the previous approach that is developed for polymer concrete, (i.e., ASTM C267 [50]). The chemical acidification test involves the immersion of concrete, mortar or cement paste specimens in a chemically prepared sulfuric acid solution in a desired pH range, typically in Stage-3. The main argument against chemical acid test is that there is no bacteria or biological process involved and therefore it does not simulate corrosion environment realistically [29, 33, 51, 52]. It essentially assumes all concretes will end up in the Stage-3 state and does not make a distinction on performance if Stage-1 or Stage-2 could be altered. However, many specifiers and researchers have used chemical acid immersion test because it is economical and straightforward to set up. At the same time,

corrosion parameters such as calcium and sulfate concentrations, and the strength reduction can be easily measured [29, 31, 53-56]. Although efforts to compare biogenic and chemical acid tests were made, these comparisons are challenging because the chemical acidification tests' pH and composition change rapidly, and the damaged cementitious systems show noticeable differences [33, 52]. In addition, it is difficult to use the chemical acidification test to explore the Stage-2 deterioration mechanisms. Nevertheless, the challenge of keeping the pHs of the exposure media consistent over time is yet to be addressed, especially in higher pHs that tend to occur at Stage-2 corrosion.

The biological growth chamber test is a traditional method to simulate MICC, which is based on recreating of a sewer environment in a closed chamber. The concrete specimens are inoculated with bacteria, and $\text{H}_2\text{S}_{(g)}$ as a primary source of nutrients [57] is continuously supplied. Several environmental features such as temperature, relative humidity, pH, H_2S concentration and inoculum of bacteria can be controlled in the chamber as shown in Figure-1.3. Since it can constantly supply nutrients for bacteria and control several environmental factors, this test can be used to simulate all three stages of MICC [5, 22, 57, 58]. Therefore, the biological chamber test is typically known as the most realistic simulation test for MICC. However, the use of poisonous H_2S gas in the laboratory is highly hazardous and requires additional safety precautions [51]. Also, the control of exposure conditions can be difficult during the long duration of the test which can take several months to over a year [37, 46, 59]. Since the biological chamber is a complex system with advanced environmental control features, it is not easily implementable in many laboratories due to safety issues and cost. Therefore, the biological chamber test is not widely used and developed as a standardized procedure.

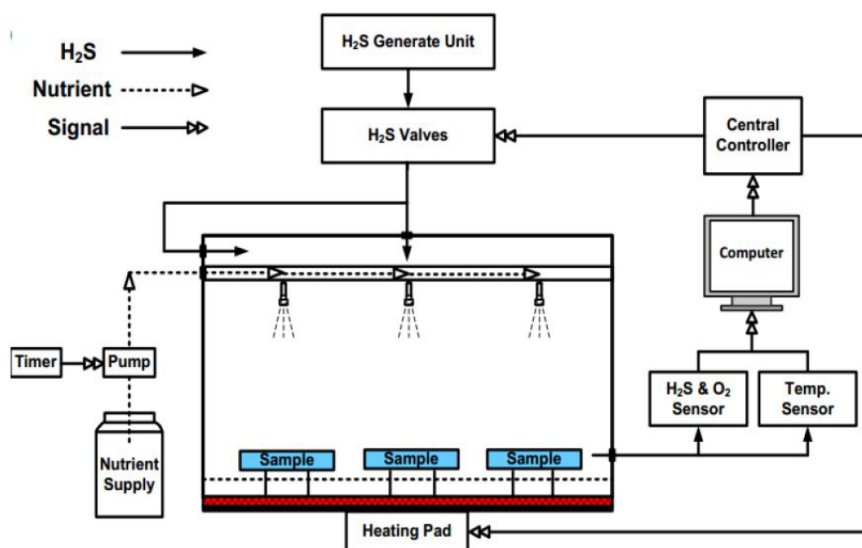


Figure-1.3: Design configuration of biological growth chamber test developed by House [37] and later used by Ding [60]

Many researchers attempted to simplify the biological chamber test, which led to the biogenic acid immersion test [21, 45, 47]. In this test, concrete, mortars or cement paste specimens are inoculated with SOB before being immersed in the nutrient-rich exposure media which can be either simulated or actual wastewater [61]. The test's main advantage is that sulfur or thiosulfate can be used as nutrients and thus poisonous H₂S is not necessary [51, 52, 62, 63]. The test's primary control is the periodic bacteria inoculation on the specimens to maintain the pH of the exposure media [52, 63, 64]. The test can be completed in weeks. As simple setup of the test is shown in Figure-1.4. Since it is more straightforward to set up while providing a realistic corrosion environment with bacterial activities being involved, this type of test becomes the best candidate to be standardized for MICC reproduction. Erbehtas et al. [63] proposed a biogenic acidification testing procedure that is more practical and economical than a biological chamber test. This test was later standardized as ASTM C1904-20 [65].

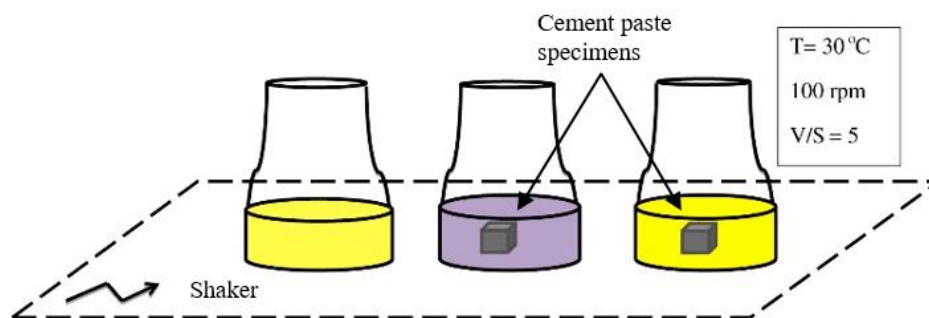


Figure-1.4: Schematic diagram of benchtop biogenic immersion test set up used by Yousefi et al. [21]. V/S represents the ratio of liquid volume to surface area of the cement paste specimens

1.3. Problem Definition and Research Objectives

Currently, three standardized testing procedures exist to study MICC of paste, mortar, or concrete. ASTM C1894-19^[66] discusses MICC products and laboratory test methods for determining the resistance to MICC. ASTM C1898^[49] provides the standard procedure for determining the chemical resistance of concrete products to acid attack. ASTM C1904^[65] provides the standard test methods for determination of the effects of biogenic acidification on concrete antimicrobial additives and/or concrete products. In all approaches, the deterioration of cementitious samples is assessed through well-defined criteria, some of which are shared by all approaches such as calcium and sulfate leaching, as well as strength reduction through ball-on-three-ball flexural testing^[67-75].

As the ASTM C1904-20 procedures use active bacteria to cause MICC, it is more challenging to implement than the ASTM C1898-20 procedure. However, there are significant concerns about the ASTM C1898-20 has several concerns. These concerns stem from the challenges associated with (1) the test setup and maintaining stable acidification conditions throughout the test duration, (2) linking the chemical deterioration to biogenic attack, (3) interpretation of the results through ball-on-three-ball (B3B) flexural strength testing conditions. This research investigates these challenges and has the following objectives.

- To develop a chemical acidification test setup that can maintain the pH of the exposure solution relatively constant during the duration of the test with no or little interference (auto-titration process).
- To use the developed chemical acidification setup to study deterioration parameters of MICC at different pH levels and for various paste compositions, as quantified by acid consumption to maintain the pH, amounts of leached calcium and sulfate from the paste specimens, and the strength reduction as measured by B3B testing.
- To study the relationship between the chemical acidification test and the theoretical systems that deteriorate due to H₂S exposure.
- To investigate the B3B test in quantifying mechanical damage in specimens that experience chemical acidification.

1.4. Thesis Organization

This thesis consists of five chapters. Chapter 1 introduces a background and literature review on the mechanisms of MICC and its primary test methods to assess the performance of concrete composites. This chapter also provides the problem definition, the objectives, and the organization of the thesis.

Chapter 2 describes the development of an automated chemical acidification test on cement paste specimens to study deterioration parameters of MICC at different pH levels and various paste compositions. This chapter also presents the relationship between the chemical acidification test and the theoretical systems that deteriorate due to H₂S exposure. Chapter 3 provides the investigation of the B3B test in quantifying mechanical damage in specimens that experience chemical acidification. Chapter 4 summarizes the findings of this thesis and provides the general conclusions. This chapter also provides suggestions for further research in automated chemical acidification tests and the flexural strength test. Additional preliminary studies that led to the development of the automated chemical acidification test setup are presented in the Appendix.

1.5.References

1. (ASCE), A.S.o.C.E., *2017 Infrastructure Report Card: A Comprehensive Assessment of America's Infrastructure*. 2017: p. 112.
2. Parker, C.D., *THE CORROSION OF CONCRETE*. Australian Journal of Experimental Biology and Medical Science, 1945. **23**(2): p. 91-98.
3. Islander, R.L., et al., *Microbial Ecology of Crown Corrosion in Sewers*. Journal of Environmental Engineering, 1991. **117**: p. 751-770.
4. Mori, T., et al., *Microbial Corrosion of Concrete Sewer Pipes, H₂S Production from Sediments and Determination of Corrosion Rate*. Water Science and Technology, 1991. **23**(7-9): p. 1275-1282.
5. Mori, T., et al., *Interactions of nutrients, moisture and pH on microbial corrosion of concrete sewer pipes*. Water Research, 1992. **26**(1): p. 29-37.
6. Grengg, C., et al., *Microbiologically induced concrete corrosion: A case study from a combined sewer network*. Cement and Concrete Research, 2015. **77**: p. 16-25.
7. Sydney, R., E. Esfandi, and S. Surapaneni, *Control Concrete Sewer Corrosion via the Crown Spray Process*. Water Environment Research, 1996. **68**(3): p. 338-347.
8. Wu, L., C. Hu, and W.V. Liu, *The Sustainability of Concrete in Sewer Tunnel—A Narrative Review of Acid Corrosion in the City of Edmonton, Canada*. Sustainability, 2018. **10**(2): p. 517.
9. Ling, A.L., et al., *High-Resolution Microbial Community Succession of Microbially Induced Concrete Corrosion in Working Sanitary Manholes*. PLOS ONE, 2015. **10**(3): p. e0116400.
10. Sand, W. and E. Bock, *Concrete corrosion in the Hamburg Sewer system*. Environmental Technology Letters, 1984. **5**(12): p. 517-528.
11. Li, X., et al., *The Ecology of Acidophilic Microorganisms in the Corroding Concrete Sewer Environment*. Frontiers in Microbiology, 2017. **8**(683).

12. Okabe, S., et al., *Succession of Sulfur-Oxidizing Bacteria in the Microbial Community on Corroding Concrete in Sewer Systems*. Applied and Environmental Microbiology, 2007. **73**(3): p. 971.
13. Saricimen, H., et al., *Durability of proprietary cementitious materials for use in wastewater transport systems*. Cement and Concrete Composites, 2003. **25**(4): p. 421-427.
14. Pomeroy, R.D. and J.D. Parkhurst, *THE FORECASTING OF SULFIDE BUILD-UP RATES IN SEWERS*. 1978: Elsevier Ltd. 621-628.
15. Droste, R.L. and R.L. Gehr, *Theory and practice of water and wastewater treatment*. 2018: John Wiley & Sons.
16. Santo Domingo, J.W., et al., *Molecular survey of concrete sewer biofilm microbial communities*. Biofouling, 2011. **27**(9): p. 993-1001.
17. Parker, C.D., *Species of Sulphur Bacteria Associated with the Corrosion of Concrete*. Nature, 1947. **159**(4039): p. 439-440.
18. Metcalf, et al., *Wastewater Engineering: Treatment and Reuse*. 2002: McGraw-Hill Education.
19. Padival, N.A., J.S. Weiss, and R.G. Arnold, *Control of Thiobacillus by Means of Microbial Competition: Implications for Corrosion of Concrete Sewers*. Water Environment Research, 1995. **67**(2): p. 201-205.
20. Ali Riza, E., O.B. Isgor, and W.J. Weiss, *Evaluating the efficacy of antimicrobial additives against biogenic acidification in simulated wastewater exposure solutions*. RILEM Technical Letters, 2019. **4**(0).
21. Yousefi, A., A. Allahverdi, and P. Hejazi, *Accelerated biodegradation of cured cement paste by Thiobacillus species under simulation condition*. International Biodeterioration & Biodegradation, 2014. **86**: p. 317-326.
22. House, M., Weiss, J., *Review of Microbially Induced Corrosion and Comments on Needs Related to Testing Procedures*. Proceedings of the 4th International Conference on the Durability of Concrete Structures, 2014.

23. Parker, C.D., *Mechanics of Corrosion of Concrete Sewers by Hydrogen Sulfide*. Sewage and Industrial Wastes, 1951. **23**(12): p. 1477-1485.
24. Carde, C., R. François, and J.-M. Torrenti, *Leaching of both calcium hydroxide and C-S-H from cement paste: Modeling the mechanical behavior*. Cement and Concrete Research, 1996. **26**(8): p. 1257-1268.
25. Mehta, P.K., *Concrete. Structure, properties and materials*. 1986.
26. Mehta, P.K. and P.J. Monteiro, *Concrete: microstructure, properties, and materials*. 2014: McGraw-Hill Education.
27. De Belie, N., et al., *Experimental research and prediction of the effect of chemical and biogenic sulfuric acid on different types of commercially produced concrete sewer pipes*. Cement and Concrete Research, 2004. **34**(12): p. 2223-2236.
28. Monteny, J., et al., *Chemical and microbiological tests to simulate sulfuric acid corrosion of polymer-modified concrete*. Cement and Concrete Research, 2001. **31**(9): p. 1359-1365.
29. Monteny, J., et al., *Chemical, microbiological, and in situ test methods for biogenic sulfuric acid corrosion of concrete*. Cement and Concrete Research, 2000. **30**(4): p. 623-634.
30. Allahverdi, A. and F. ŠKVÁRA, *Acidic corrosion of hydrated cement based materials*. Ceramics– Silikáty, 2000. **44**(4): p. 152-160.
31. Emmanuel, K.A. and H.R. Sami, *Response of Concrete to Sulfuric Acid Attack*. ACI Materials Journal. **85**(6).
32. Gutberlet, T., H. Hilbig, and R. Beddoe, *Acid attack on hydrated cement—Effect of mineral acids on the degradation process*. Cement and Concrete Research, 2015. **74**: p. 35-43.
33. Huber, B., et al., *Comparative analysis of biogenic and chemical sulfuric acid attack on hardened cement paste using laser ablation-ICP-MS*. Cement and Concrete Research, 2016. **87**: p. 14-21.

34. Reardon, E., *An ion interaction model for the determination of chemical equilibria in cement/water systems*. Cement and Concrete Research, 1990. **20**(2): p. 175-192.
35. Warren, C. and E. Reardon, *The solubility of ettringite at 25 C*. Cement and Concrete Research, 1994. **24**(8): p. 1515-1524.
36. Gabrisova, A., J. Havlica, and S. Sahu, *Stability of calcium sulphoaluminate hydrates in water solutions with various pH values*. Cement and Concrete Research, 1991. **21**(6): p. 1023-1027.
37. House, M. *Using biological and physico-chemical test methods to assess the role of concrete mixture design in resistance to microbially induced corrosion*. 2013.
38. Joseph, A.P., et al., *Surface neutralization and H₂S oxidation at early stages of sewer corrosion: influence of temperature, relative humidity and H₂S concentration*. Water research, 2012. **46**(13): p. 4235-4245.
39. Erbehtas, A.R., *Development of Practical Accelerated Testing Protocols for the Performance Evaluation of Concrete against Microbially Induced Corrosion of Concrete*. 2018, Oregon State University.
40. Roberts, D., et al., *Quantifying microbially induced deterioration of concrete: initial studies*. International Biodeterioration & Biodegradation, 2002. **49**(4): p. 227-234.
41. Alexander, M. and C. Fourie, *Performance of sewer pipe concrete mixtures with portland and calcium aluminate cements subject to mineral and biogenic acid attack*. Materials and structures, 2011. **44**(1): p. 313-330.
42. Nica, D., et al., *Isolation and characterization of microorganisms involved in the biodeterioration of concrete in sewers*. International biodeterioration & biodegradation, 2000. **46**(1): p. 61-68.
43. Bielefeldt, A., et al., *Bacterial kinetics of sulfur oxidizing bacteria and their biodeterioration rates of concrete sewer pipe samples*. Journal of Environmental Engineering, 2010. **136**(7): p. 731-738.

44. House, M., et al., *Concrete Resistance to Sulfuric Acid Immersion: The Influence of Testing Details and Mixture Design on Performance as It Relates to Microbially Induced Corrosion*. *Advances in Civil Engineering Materials*, 2019. **8**(1): p. 544-557.
45. Huber, B., et al., *Characterization of sulfur oxidizing bacteria related to biogenic sulfuric acid corrosion in sludge digesters*. *BMC Microbiology*, 2016. **16**(1): p. 153.
46. Huber, B., et al., *Evaluation of concrete corrosion after short- and long-term exposure to chemically and microbially generated sulfuric acid*. *Cement and Concrete Research*, 2017. **94**: p. 36-48.
47. Soleimani, S., O.B. Isgor, and B. Ormeci, *Effectiveness of *E. coli* Biofilm on Mortar to Inhibit Biodegradation by Biogenic Acidification*. *Journal of Materials in Civil Engineering*, 2016. **28**(4): p. 04015167.
48. Pomeroy, R.D., *Pomeroy's Model of Corrosion Rate*. U.S. Environmental Protection Agency, 1974.
49. *New ASTM Standard Test Methods for Determining the Chemical Resistnace of Concrete Products to Acid Attack*. 2020, ASTM International: West Conshohocken, PA.
50. *Standard Test Methods for Chemical Resistance of Mortars, Grouts, and Monolithic Surfacing and Polymer Concretes*. 2020, ASTM C267: ASTM International, West Conshohocken, PA.
51. Peyre Lavigne, M., et al., *An innovative approach to reproduce the biodeterioration of industrial cementitious products in a sewer environment. Part I: Test design*. *Cement and Concrete Research*, 2015. **73**: p. 246-256.
52. Erbehtas, A.R., O. Isgor, and W. Weiss, *Comparison of Chemical and Biogenic Acid Attack on Concrete*. *ACI Materials Journal*, 2020. **117**.
53. Hewayde, E., et al., *Using concrete admixtures for sulphuric acid resistance*. *Proceedings of the Institution of Civil Engineers - Construction Materials*, 2007. **160**(1): p. 25-35.

54. Soleimani, S., O. Isgor, and B. Ormeci, *Resistance of biofilm-covered mortars to microbiologically influenced deterioration simulated by sulfuric acid exposure*. Cement and Concrete Research, 2013. **53**: p. 229-238.
55. Hewayde, E., et al., *Effect of Mixture Design Parameters and Wetting-Drying Cycles on Resistance of Concrete to Sulfuric Acid Attack*. Journal of Materials in Civil Engineering, 2007. **19**(2): p. 155-163.
56. Larreur-Cayol, S., A. Bertron, and G. Escadeillas, *Degradation of cement-based materials by various organic acids in agro-industrial waste-waters*. Cement and Concrete Research, 2011. **41**(8): p. 882-892.
57. Sand, W., E. Bock, and D. White. *Biotest system for rapid evaluation of concrete resistance to sulfur-oxidizing bacteria*. 1987.
58. Ding, L., W.J. Weiss, and E.R. Blatchley, *Effects of Concrete Composition on Resistance to Microbially Induced Corrosion*. Journal of Environmental Engineering, 2017. **143**(6): p. 04017014.
59. Ehrich, S., et al., *Biogenic and Chemical Sulfuric Acid Corrosion of Mortars*. Journal of Materials in Civil Engineering, 1999. **11**(4): p. 340-344.
60. Ding, L., *Assessing the performance of antimicrobial concrete admixtures in concrete subjected to microbially induced corrosion*. 2015: Purdue University.
61. Gutiérrez-Padilla, M.G.D., et al., *Biogenic sulfuric acid attack on different types of commercially produced concrete sewer pipes*. Cement and Concrete Research, 2010. **40**(2): p. 293-301.
62. Matthieu, P.L., et al., *Innovative approach to simulating the biodeterioration of industrial cementitious products in sewer environment. Part II: Validation on CAC and BFSC linings*. Cement and Concrete Research, 2016. **79**.
63. Erbehtas, A.R., O.B. Isgor, and W.J. Weiss, *An accelerated testing protocol for assessing microbially induced concrete deterioration during the bacterial attachment phase*. Cement and Concrete Composites, 2019. **104**: p. 103339.
64. Vincke, E., et al., *A new test procedure for biogenic sulfuric acid corrosion of concrete*. Biodegradation, 1999. **10**(6): p. 421-428.

65. *Standard Test Methods for Determination of the Effects of Biogenic Acidification on Concrete Antimicrobial Additives and/or Concrete Products*. 2020, ASTM C1904: ASTM International, West Conshohocken, PA.
66. *Standard Guide for Microbially Induced Corrosion of Concrete Products*. 2019, ASTM C1894-19: ASTM International, West Conshohocken, PA.
67. Fu, T., et al., *The Influence of Cellulose Nanocrystals on the Hydration and Flexural Strength of Portland Cement Pastes*. *Polymers (Basel)*, 2017. **9**(9).
68. Fu, T. and W. Weiss, *The Ball-on-Three-Ball (B3B) Test – Application to Cement Paste and Mortar*. *Advances in Civil Engineering Materials*, 2020. **9**(1): p. 128-142.
69. Qiao, C., P. Suraneni, and J. Weiss, *Damage in cement pastes exposed to NaCl solutions*. *Construction and Building Materials*, 2018. **171**: p. 120-127.
70. Qiao, C., P. Suraneni, and J. Weiss, *Flexural strength reduction of cement pastes exposed to CaCl₂ solutions*. *Cement and Concrete Composites*, 2018. **86**: p. 297-305.
71. Cao, Y., et al., *Performance-enhanced cementitious materials by cellulose nanocrystal additions*. *Production and Applications of Cellulose Nanomaterials*, 2013. **2**.
72. Cao, Y., et al., *The influence of cellulose nanocrystal additions on the performance of cement paste*. *Cement and Concrete Composites*, 2015. **56**: p. 73-83.
73. Cao, Y., et al., *The relationship between cellulose nanocrystal dispersion and strength*. *Construction and Building Materials*, 2016. **119**: p. 71-79.
74. Börger, A., P. Supancic, and R. Danzer, *The ball on three balls test for strength testing of brittle discs: stress distribution in the disc*. *Journal of the European Ceramic Society*, 2002. **22**(9): p. 1425-1436.
75. Börger, A., P. Supancic, and R. Danzer, *The ball on three balls test for strength testing of brittle discs: Part II: analysis of possible errors in the strength*

determination. Journal of the European Ceramic Society, 2004. **24**(10): p. 2917-2928.

2. AUTOMATED CHEMICAL ACID IMMERSION TEST OF CEMENTITIOUS MATERIALS

2.1. Introduction

Currently, two standardized testing procedures exist to study MICC of cementitious materials such as paste, mortar, or concrete. ASTM C1898 ^[1] provides the standard procedure for determining the chemical resistance of concrete products to chemical acid attack. ASTM C1904 ^[2] provides the standard test methods for determination of the effects of biogenic acidification on concrete antimicrobial additives and/or concrete products. In both approaches, the deterioration of cementitious samples is assessed through well-defined criteria, some of which are shared by both methods such as the amount of calcium and sulfate leaching, as well as reduction in strength through ball-on-three-ball (B3B) flexural testing ^[3-13].

As the ASTM C1904 procedures use active bacteria to induce MICC, it is more challenging to implement than the ASTM C1898 procedure, which is based on chemical (sulfuric) acid immersion. However, there are significant concerns about the ability and validity of the ASTM C1898 test to study MICC. One of the most difficult tasks in chemical acid immersion tests for cementitious materials is to keep the pH of the exposure solution at constant and stable, which is challenging due to leaching from the deteriorated cementitious matrix. As shown in previous studies^[12, 14-20] shortly after immersion of cementitious specimens in sulfuric acid solutions, the leaching of calcium and sulfate ions start, and the pH of the exposure solution sharply increases, which makes it impossible to maintain the pH at the desired level for the duration of the experiment. An example of this behavior is shown in Figure 2.1, which reports the change in pH of the sulfuric acid solutions that were initially at pH2 and pH5. It is clear that within few hours, the pH of the solutions increases sharply. As the pH of the solutions needs to be maintained stable for weeks, this effect poses a challenge to acid immersion testing.

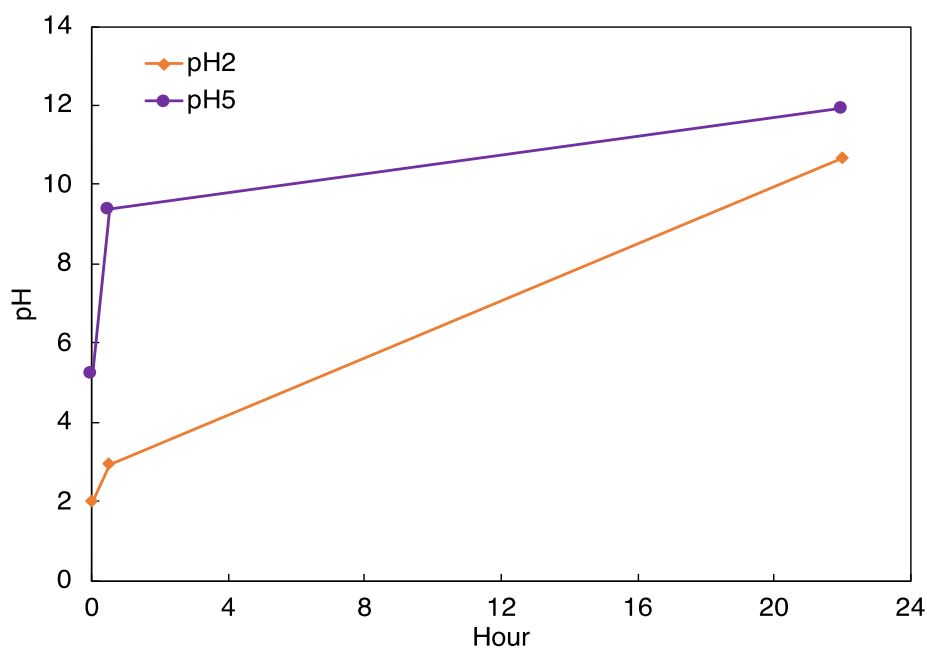


Figure-2.1: Rapid rise of pH within minutes to hours after cement paste specimens were immersed in sulfuric acid solutions that were initially at pH2 and pH5

As part of this research, we conducted preliminary studies to explore if the pH of the solution can be maintained constant and stable. These preliminary and exploratory studies are presented in the Appendix. These studies included the investigation of the effect of the following factors on the pH of the exposure solution: (1) the solution-to-sample volume ratio, (2) exposure of the test setup to the atmosphere during the experiments, (3) using glass vs. plastic containers for keeping the exposure solution and the test specimens, (4) using a mixture of sulfuric acid and a buffer solution to test the hypothesis that increasing buffer capacity might maintain pH of the solution during the experiments. As shown in the Appendix, none of these approaches helped maintain the pH of the exposure solutions stable, therefore, a new approach to chemical acid immersion testing is needed.

This paper presents such an approach that is based on automatically titrating the exposure solution with sulfuric acid based on the active measurement of the pH response of the system. The new approach is intended to maintain the pH of the exposure solution relatively constant during the duration of the test with no or little interference. The new

testing approach is shown to be a useful tool to study deterioration parameters of MICC at different pH levels and for various paste compositions, as quantified by acid consumption to maintain the pH, amounts of leached calcium and sulfate from the paste specimens, and the strength reduction as measured by B3B testing. The new approach is also used to investigate the relationship between the chemical acidification test and the theoretical systems ^[21, 22] that calculate the rate of deterioration due to H₂S exposure.

2.2. Materials and Methods

2.2.1. Overview

Two types of cement paste mixtures, ordinary portland cement (OPC), and OPC with the antimicrobial additive (AM), were prepared to be exposed to sulfuric acid solutions. OPC specimens were immersed in the solutions with pH1, 2, 3, and 4 while AM specimens were only exposed to pH2 and pH3 in this experiment. AM specimens were not tested in pH1 and pH4. In the past research, the effectiveness of AM admixture has been tested in Stage-3 corrosion where pH1 is within the range. Meanwhile, corrosion is not significant between pH3 and pH4 even for mixtures ^[12, 23] without AM and therefore, it is hard to determine the performance of the admixture in pH higher than 3.

For each pH cell, 15 paste specimens were immersed in the solution at the beginning of the test. Seven or eight specimens were removed from the solutions after 21 and 42 days to test their flexural strength. Additional 20 specimens were also prepared for each group of mixtures to be immersed in control cells that have calcium hydroxide solution (limewater) to preserve the leaching of calcium. Limewater was prepared with calcium hydroxide concentration 2g/L as stated in AASHTO TP119-15 (2019) ^[24]. The first five specimens from control group were used for initial flexural strength before acid immersion. The rest of 15 control specimens were immersed in limewater, and they were also removed after 21 and 42 days for testing their flexural strength.

During immersion, the specimens were expected to leach calcium and sulfate ions and raise the pH in the solution. Therefore, these ions are monitored in the solution during the experiments. To maintain the desired pH in each pH cell throughout the experiment, an automated titration procedure was developed. This new approach is based on automatically titrating the exposure solution with sulfuric acid based on active measurement of the pH response of the system. The detailed configuration of the setup is described in section 2.2.4.

2.2.2. Preparation of paste specimens

Type I/II Ordinary Portland Cement in compliance with ASTM C150/C150M-20 ^[25] was used for cement paste in both mixtures with water to cement ratio (w/c) by mass of 0.42. The chemical composition of the OPC is provided in Table-2.1. Silane quaternary ammonium chloride (SQA or Si-QAC) aqueous salt solution containing 3.6% active ingredient (3-trihydroxysilyl) was used as the antimicrobial additive. The effectiveness of the antimicrobial additive was investigated in the past research ^[12, 13, 23, 26, 27]. For the mixture with additive, the total amount of antimicrobial added to the mixture is counted as water when calculating w/c ratio. Table-2.2 summarizes the information of mixture designs.

Table-2.1: Oxide Composition of the Type I/II ordinary portland cement (OPC) in compliance with ASTM C150

Components	Mass (%)
Silicon dioxide (SiO ₂)	19.9
Aluminum oxide (Al ₂ O ₃)	4.6
Ferric oxide (Fe ₂ O ₃)	3.2
Calcium oxide (CaO)	62
Magnesium oxide (MgO)	3.8
Sulfur trioxide (SO ₃)	2.8
Loss on ignition (LOI)	1.6
Insoluble residue (IR)	0.7
Alkalies (Na ₂ O+0.658*K ₂ O)	0.57
Tricalcium silicate (C ₃ S)*	57
Dicalcium silicate (C ₂ S)*	14
Tricalcium aluminate (C ₃ A)*	7
Tetracalcium aluminoferrite (C ₄ AF)*	10
Limestone (CaCO ₃ – 86%)	1

*Cement chemistry notation: C = CaO, S = SiO₂, A = Al₂O₃, F = Fe₂O₃

Table-2.2: Summary of Mixture Designs

Mixture Name	w/c ratio	Antimicrobial admixture (g/kg of cement)	Topically Treated
OPC	0.42	-	
AM	0.42	7.5	Yes

Vacuum mixing was performed using the Twister Evolution mixer (Renfert, St. Charles, IL) as described by Erbehtas et al. ^[12, 13] and Fu et al. ^[7] and adopted in ASTM C1904 ^[2]. The vacuum mixer is used to reduce entrapped air in cement paste while mixing. The mixer was operated at a speed of 400 rpm under 80% vacuum for two 90 seconds periods. Between two mixing periods, the mixer bowl's inner surface and the blade were scrapped with a spatula for approximately 30 seconds to improve homogeneity. The fresh paste was then poured into cylindrical molds with 50.8 ± 1.5 mm diameter and 101.6 ± 1.5 mm height. The specimens were at a temperature $23^{\circ}\text{C} \pm 2^{\circ}\text{C}$ for 28 days in a sealed condition. After curing, the cylinders were demolded and sliced into disks with thickness 2.65 ± 0.25 mm by using diamond blade wet saw. The middle 60 mm portion of the cylinder was used in slicing and the outer 20 mm at each end of the cylinder was discarded to avoid defects.

The AM specimens were also topically treated with the same antimicrobial admixture diluted to 75% by weight. The antimicrobial solution was sprayed onto the specimen surface at two times separated by approximately five minutes of air drying to create two layers of treatment. The appearance of the topically treated specimens were not visually significant. The total volume of the solution applied per surface area was recorded as $0.178\text{mL}/\text{cm}^2$.

2.2.3. Preparation of the initial exposure and titration solutions

Four pH exposure conditions were investigated in this study, i.e., pH1, 2, 3, and 4. These solutions were prepared by using 98% concentrated sulfuric acid and Type-IV DI water. 98% concentrated sulfuric acid was incrementally poured (i.e., 1 mL at a time with a pipette) into 3100 mL of Type-IV DI water. The pH of the solution was measured after

each injection of 98% concentrated sulfuric acid. The process continued until the pH of the solution reached the desired pH level. The targeted starting volume of the exposure solution in each cell was calculated using a solution-volume-to-total-specimen-surface-area ratio of 4.67, following ASTM 1898-20^[1]. For each paste specimen used in this experiment, the surface area was 44.76 cm²; therefore, for a cell with 15 paste specimens, 3135.44 cm³ (or mL) of initial exposure solution was prepared. The container for each cell was selected to be significantly larger than this initial volume so that additional acid during the titration process did not overflow. A typical cell with specimens and initial exposure solution are shown in Figure-2.2. Note that specimens are organized in a way that both of their exposed surfaces are exposed to the solution by having a polypropylene mesh lifting the specimens from the bottom of the container.



Figure-2.2: A typical cell with specimens in the initial exposure solution.

In addition to the initial exposure solution, a concentrated sulfuric acid solution with a pH of 0.1 was prepared to be used as the titration solution. 98% concentrated sulfuric acid and Type-IV DI water were used to prepare this solution. Before dividing into four graduated cylinders, the titration solution was prepared in one container for consistency across different cells. 98% concentrated sulfuric acid was incrementally poured (i.e., 10 mL at a

time with a pipette) into approximately 3800 mL of Type-IV DI water. The pH of the solution was measured after each injection of 98% concentrated sulfuric acid. The process continued until the pH of the solution reached pH level of 0.1. The total volume of the titration solution, initially at 3800 mL, became slightly over 4000mL due to the incremental addition of 98% concentrated sulfuric acid. The pH0.1 titration solution was divided into four graduated cylinders with each storing 1000 mL. The volume indicator in the graduated cylinders was used to track the consumption of titration solution during the experiments. Each graduated cylinder was incorporated into each set up of automated-titrator. Both the titration and exposure solutions were placed in a secondary container for safety. The auto-titration setup is explained in the following section.

2.2.4. Auto-titration setup and operation

The schematic of the auto-titration setup is presented in Figure-2.3. The system contains eight components:

1. Control Panel/Pump – BL7916 (Hanna Instruments, Smithfield, RI, USA) – a combination of a control panel and a pump as in a single unit.
2. Titration solution container – 1000mL graduated cylinder to store concentrated sulfuric acid solution with pH=0.1 that will be dosed into exposure solution and to use in tracking the solution volume change during operation.
3. Specimens container – a polypropylene container that keeps the cement paste specimens in the exposure sulfuric acid solution of desired pHs (pH1, 2, 3 and 4 for this experiment). A polypropylene mesh was placed at the bottom of the container to lift the specimens so that their surface area is uniformly exposed to acid solution.
4. pH electrode – an electrode is connected to the pH controller to constantly measure the pH of the exposure solutions.
5. Automatic overhead stirrer – BDC250 (Caframo Limited, Georgian Bluffs, Ontario, Canada) overhead stirrer is constantly run at 1000rpm about the center of the exposure solution.

6. Automatic data logger – SQ2010 (Grant Instrument, Beaver Falls, PA, USA) is a portable data logger that records the pH data read by the pH controller (the first component of this setup) and logs into the computer.
7. Tubing – the tubing for this setup was designed in three segments.
 - a. Hose-1 – connects the pump (the first component) and the titration solution container (the second component).
 - b. Hose-2 – connects the pump and the exposure container (the third component) to inject concentrated acid solution accordingly to keep the pH consistent over time.
 - c. Hose-3 – diverges the flow from the pump back into the titration solution container to reduce the dosing so that potential overdosing of the concentrated titration acid in the exposure container can be avoided.
8. Clamp – provides additional control of the titration solution dosage by compressing the opening of Hose-2 to reduce the flow of acid into the exposure container.

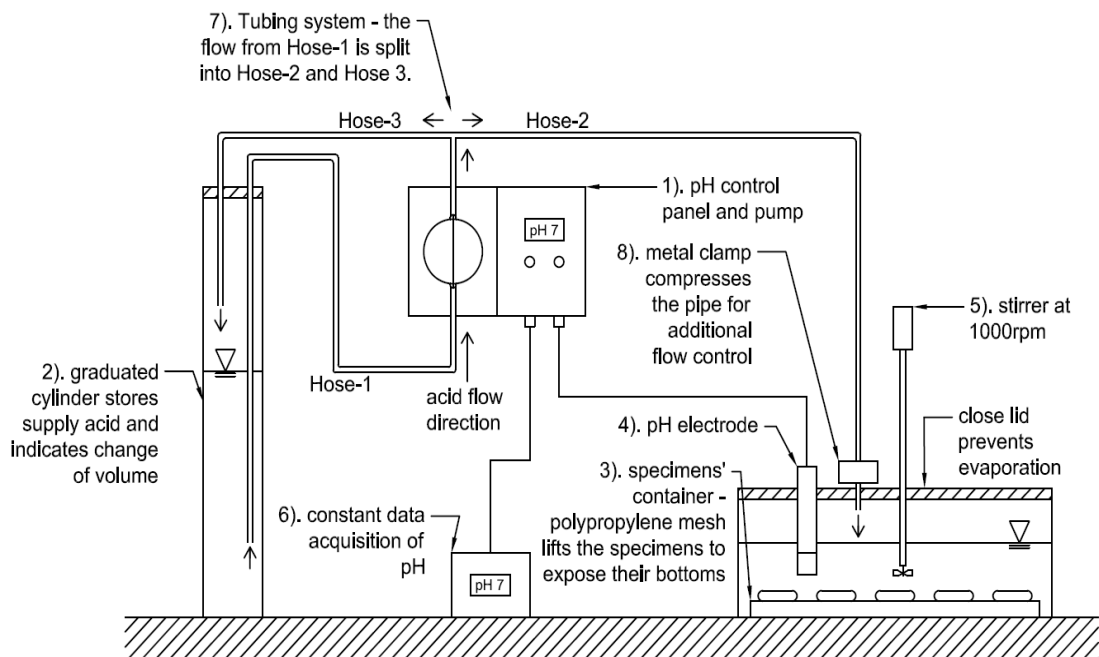


Figure-2.3: Diagram of a pH Controller Setup

The pH controller pumps and injects titration solution once the pH in the exposure container goes above the setpoint. This draws back the pH in the exposure container again

to the setpoint (e.g., for the exposure solution with setpoint pH5, when it rose to pH5.2, the pH controller dosed titration solution with pH=0.1, which reduced the pH of the exposure solution back to about 4.8.). The fluctuation between the lower and upper end of this range is recorded constantly. A portable data logger (Grant Instrument, Beaver Falls, PA) that can measure voltage, resistance, and current output, is used to measure the current output from the pH controller. The pH controller generates electrical current (mA) that resonates the reading of pH in the solution over time (i.e., the current increases as the pH increases and vice versa). The data logger constantly collects the current output and transfers the data to the computer. The current values are then converted to display as pH values, which are plotted against time so that the fluctuation of pH can be monitored on the computer screen.

Before the actual experiment was launched, a trial was operated for 24 hours to observe whether the pH controller was able to adjust in desired pH (i.e. pH2 and pH5). Figure-2.4 shows that the pH level in both pH2 and pH5 solutions were consistent over time. pH2 fluctuated between pH1.99 and pH2.15. The measurement in the pH5 solution fluctuated between pH4.83 and pH5.31. Compared to the rise of pH in the preliminary study discussed in Appendix chapter, the consistency in pH controlled by the pH controller was significantly improved.

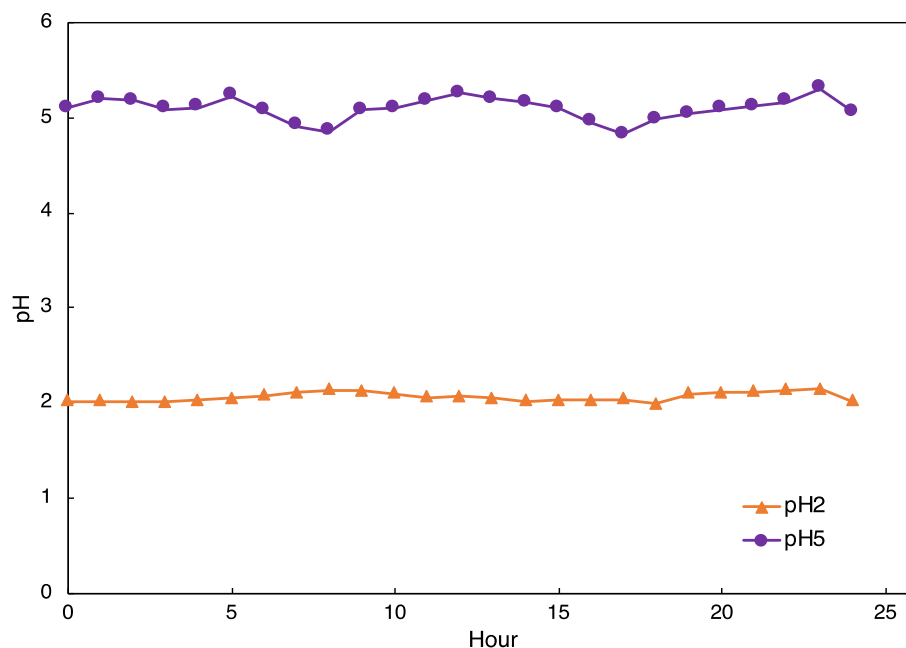


Figure-2.4: pH monitored for 24 hours during trial by using automated pH controller at initial pH level 2 and 5

2.2.5. Calcium ion concentration measurement

When cement paste specimens are immersed in sulfuric acid solution, decalcification from the specimens occurs and calcium ions are leached into the solution. To measure calcium ion concentration, a combination of calcium ion selective electrode (ISE) (Hanna Instruments, Smithfield, RI) was connected to a benchtop multi-parameter (Thermo Fisher, Waltham, MA). Since the concentration can be measured by dipping the tip of the electrode, it was simple and easy to measure frequently. The change of concentration over time can determine the rate of calcium leaching from the specimens.

2.2.6. Sulfate ion concentration measurement

Sulfate concentration was measured by a sulfate portable photometer (Hanna Instruments, Smithfield, RI). The device used turbidimetric method similar to EPA375.4 ^[28], a standard procedure by National Environmental Methods Index (NEMI). Barium chloride powder was mixed with a sample of the exposure solution to form barium sulfate, which caused turbidity in the solution which was then measured by photometer with wavelength 466nm.

Since the sulfate photometer used in this experiment can only measure between 0 to 150 mg/L, the sample solutions extracted from the exposure container were diluted from 50 to 300 times. The actual concentration was then back calculated by using molar concentration in Equation-2.1.

$$M_1V_1 = M_2V_2 \quad \text{Equation-2.1}$$

where, M_1 is the initial concentration, V_1 is the initial volume, M_2 is the final concentration, and V_2 is the final volume.

2.2.7. Acid consumption

The rate of titration solution being dosed into the exposure solution was measured by the volume indicator in the graduated cylinder that stored titration solution of pH0.1. The rate of acid consumption will be correlated with the rate of calcium leaching to determine the rate of corrosion of the specimens exposed to different pH levels.

2.2.8. Visual observation on the specimens and the exposure solutions

Half of the specimens were removed from each solution after 21 and 42 days to be tested for flexural strength (i.e., seven specimens after 21 days and eight specimens after 42 days were removed from each medium to be tested for flexural strength). The specimens were brushed with stiff-bristle brush to remove loose materials on the specimens' surface. The specimens were then rinsed with tap water for approximately 10 seconds before being patted with a paper towel and air-dried for 30 minutes. Description of the acid attack on the specimens, the color of the solution and the formation of sediments were recorded. After air-drying, the B3B flexural strength test was eventually performed.

2.2.9. The ball-on-three-ball (B3B) flexural strength test

The B3B test method has been used to evaluate the strength of ceramic ^[29-32], bone ^[33], and later in cementitious materials ^[5-9, 11-13]. The B3B test uses thin-disk shaped specimens,

which can be prepared in several replicates in a shorter amount of time by sectioning a concrete or cement paste cylinder. This improves statistical reliability of the test. In addition, due to the specimen's geometry and bi-axial loading state, it is sensitive to cracks occurred in in-plane direction [3, 4, 12, 13, 31] and therefore, strength change in specimens exposed to slightly different environments (e.g., solutions of pH3 and pH4) is detectable [8, 9, 12, 13].

The device consists of three balls that provide base support and a central ball on the top that is used to provide loading. The disk-shaped specimen is placed on three balls, which are positioned in 120° from each other under the specimen as shown in Figure-2.5. To help center the specimen, two positioning steel pins are used as shown in Figure-2.5. After the specimen is positioned in the center, the positioning pins are carefully removed. The fourth ball is then loaded over the top at the center of the specimen initially at 2.5 mm/min and later at 0.5 mm/min until it fails. A load cell is used for the maximum load at failure (or the peak load). The thickness is measured at three points at the failure plane using a digital caliper (Johnson, Mequon, WI) with 0.01 mm precision and averaged. The recorded peak load and the averaged thickness are used to calculate the flexural strength of the specimens by using Equation-2.2, the original equation developed in Börger et al. [3].

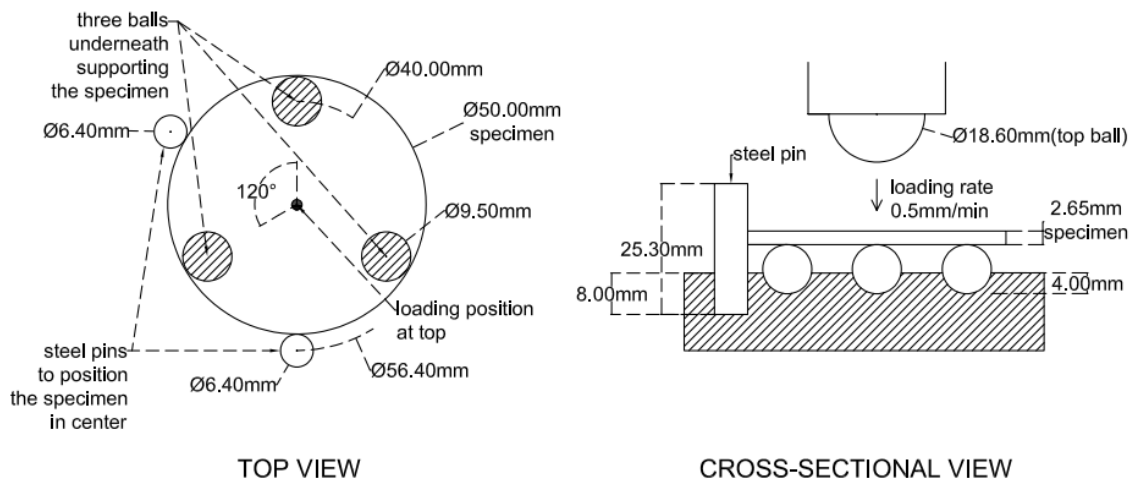


Figure-2.5: Ball-on-three-ball test setup

$$\sigma = f(\alpha, \beta, \nu) \frac{F}{t^2} \quad \text{Equation-2.2}$$

where σ is the flexural strength, α and β are the geometry parameters, ν is the Poisson's ratio, F is the peak load and t is the thickness of the specimen [3]. The geometry factor is calculated by equation-2.3 to equation-2.5 [3]:

$$f(\alpha, \beta, \nu) = C_0 + \frac{(C_1 + C_2\alpha + C_3\alpha^2 + C_4\alpha^3)(1 + C_6\beta)}{1 + C_5\alpha} \quad \text{Equation-2.3}$$

$$\alpha = \frac{t}{R} \quad \text{Equation-2.4}$$

$$\beta = \frac{R_a}{R} \quad \text{Equation-2.5}$$

In this experiment, R_a and R were 20.6 mm and 25.4 mm respectively. The specimens' geometry tested in this paper followed ASTM C1904-20 [2]. Therefore, the Poisson's ratio for cement paste specimens in this test was estimated to be 0.2 [3], and the six coefficients in $f(\alpha, \beta, \nu)$ became $C_0 = -12.354$, $C_1 = 15.549$, $C_2 = 489.2$, $C_3 = -78.707$, $C_4 = 52.216$, $C_5 = 36.554$, $C_6 = 0.082$.

2.3. Results

2.3.1. Performance of the auto-titration setup in pH stabilization

Figure-2.6 shows the average pH of 24 hours of pH data for the four different pH cells over a 42-day period. All cells maintained the pH relatively stable. The cell in pH4 encountered a relative fluctuation in the early days of immersion. It was observed that maintaining the pH stable was easier for lower pH setpoints such as pH1 and 2.

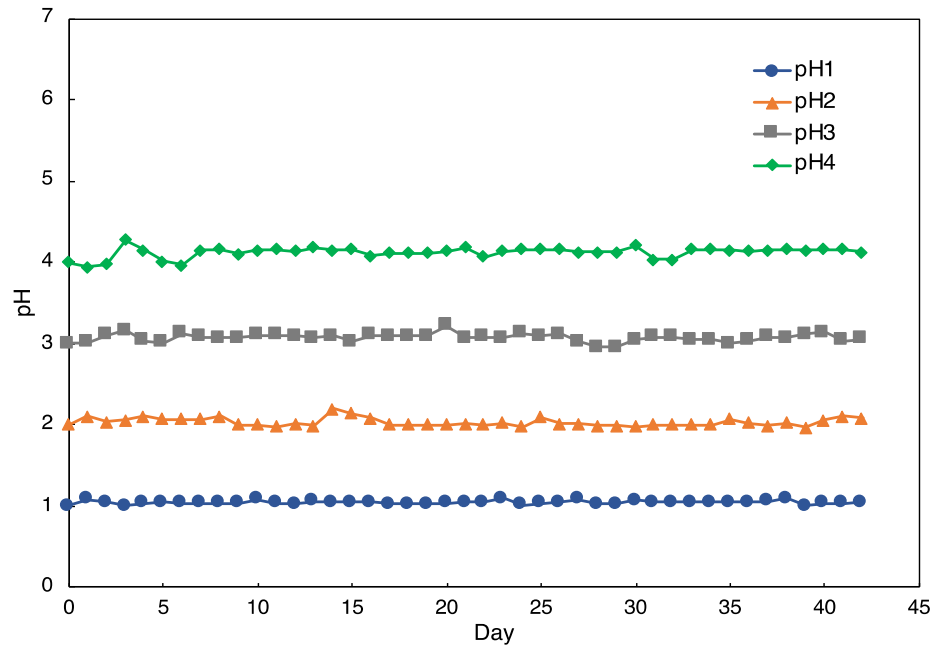


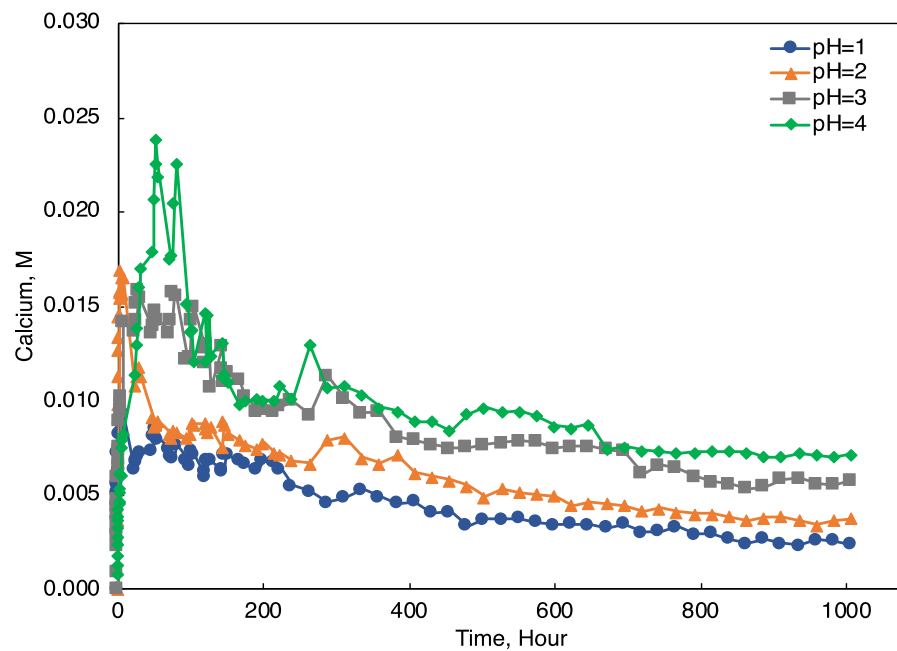
Figure-2.6: Average of 24-hours pH data collected by pH data logger.

2.3.2. Calcium ion concentration

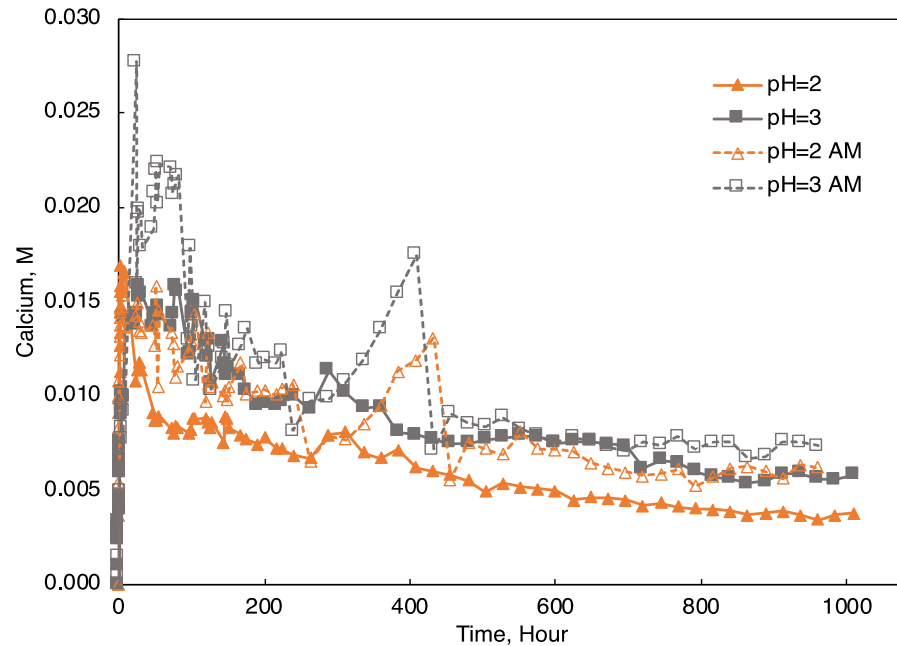
Figure-2.7 shows the concentration of calcium measured periodically throughout the immersion period. Calcium concentration was the lowest in pH1 with its peak at 0.010 M and the highest in pH4 with its peak at 0.024 M. The higher the pH of the solution, the more concentrated calcium ions present in the solution. Initially, this might appear counterintuitive as it is expected that larger amount of calcium would leach from specimens in low pH cells. However, since the acidification is maintained as a result of continuous sulfuric acid injection, the solution is always abundant in sulfate ions, which react with the leached calcium ions from the solution to form gypsum. Therefore, the acid consumption is likely a better indicator of calcium leaching than the free calcium ion content in the solution.

All four cells projected a similar trend that a sudden upward and downward movement occurred in the early hours until about hour 200 (approximately after 8 days) where a more consistent but declining slope appeared during the rest of the immersion period. The early

spike of concentration in Figure-2.7 indicates that fresh cement paste specimens were leaching calcium containing compounds, mainly calcium hydroxide but also other phases like C-S-H, with an accelerated rate before leveling off. This can be explained by the early formation of corroded layer on the specimens' surface that deters the additional leaching of calcium ions from undamaged inner portion of the specimens, an observation that was also made in earlier studies [12, 13, 34]. Figure-2.7(b) shows that the calcium concentration tends to be higher in AM specimens cells than OPC counterparts.



(a)



(b)

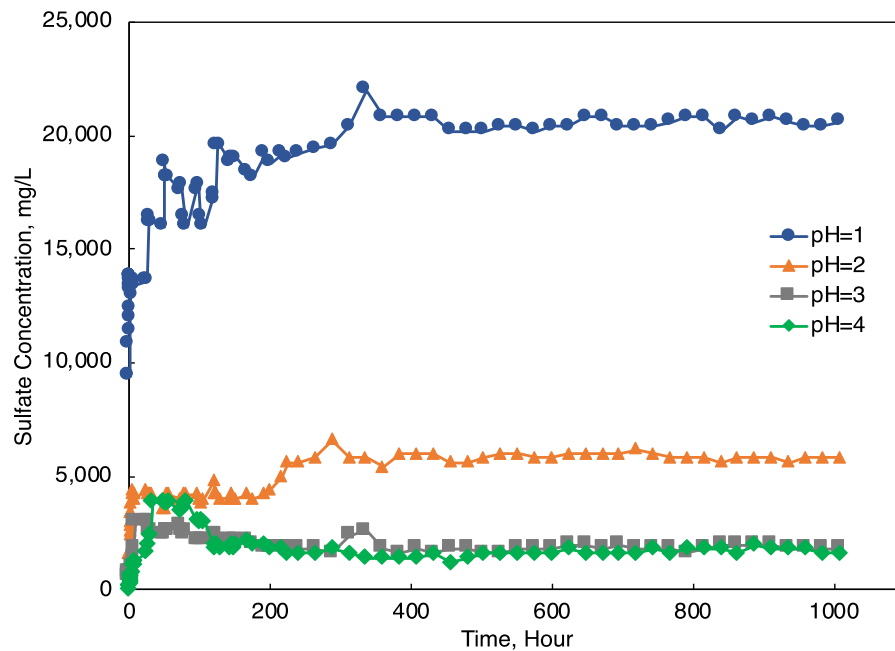
Figure-2.7: Calcium concentration in molarity (M) measured in specimens containers (a) with four different pHs for over 1000 hours (or) 42 days, and (b) in comparison of OPC and AM

2.3.3. Sulfate ion concentration

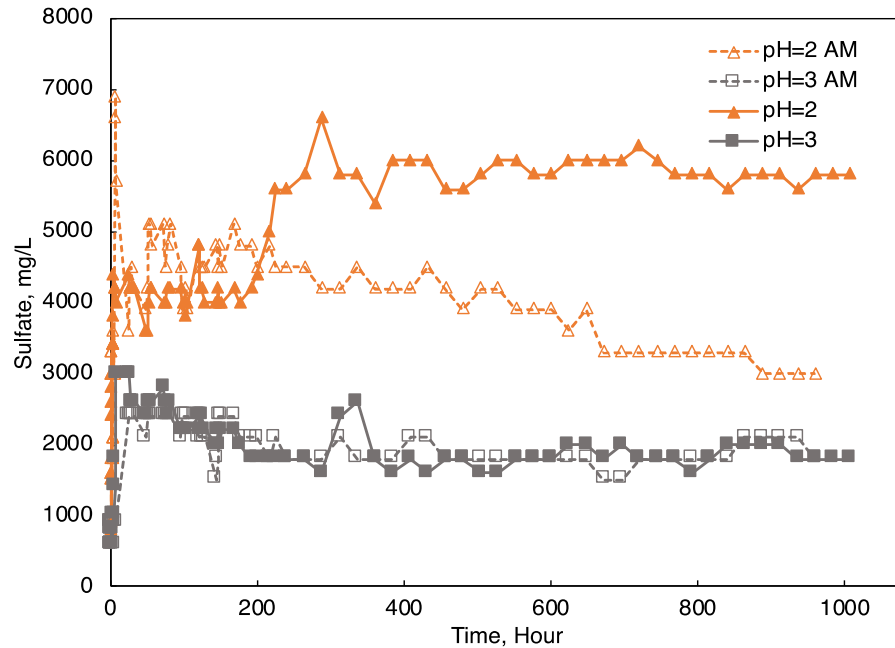
Sulfate concentration in the exposure solutions with four different pHs were measured. Figure-2.8 shows the actual concentration of sulfate ions in mg/L converted from diluted concentration data during measurement. As shown in Figure-2.8, the solution with higher pH tends to have lower concentration of sulfate ions. The highest concentration occurred in pH1 cell with around 20 kg/L and the lowest concentration in pH4 cell with approximately 1.75 kg/L throughout much of the immersion period. The pH3 cell contained the amount of sulfate ions slightly higher to pH4 cell over time while pH2 cell stabilized around 5 kg/L.

The concentration of sulfate ions increased exponentially for the about 300 hours (about 12 days) in pH1 and pH2 cells, and approximately 120 hours (5 days) in pH3 and pH4 cells before a more stable trend was projected for the rest of the immersion period in all four

containers. This can be explained by the pH controller's more frequent and faster dosing of sulfuric acid in the early days of the test. This indicates the possibility of the specimens' solution consuming more acid to counter intense alkalinization by the fresh cement paste specimens in the early part of the test as discussed in the previous section. As the pH controller kept injecting sulfuric acid, the amount of sulfate ions increased until the reaction between calcium and sulfate ions reached the equilibrium. Figure-2.8(b) shows that the sulfate concentration in AM cell is lower in pH2 but the difference in pH3 is not significant.



(a)

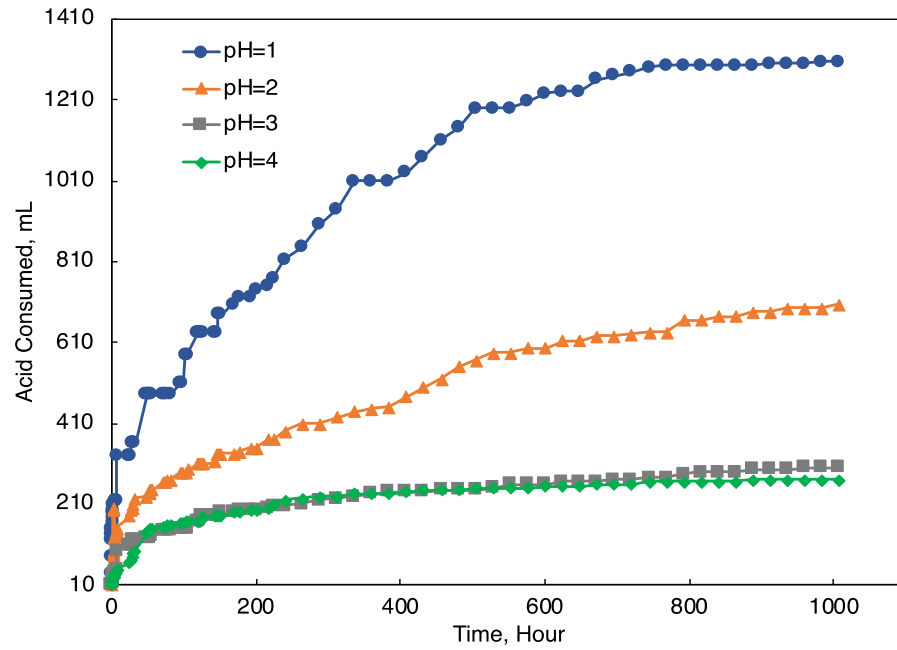


(b)

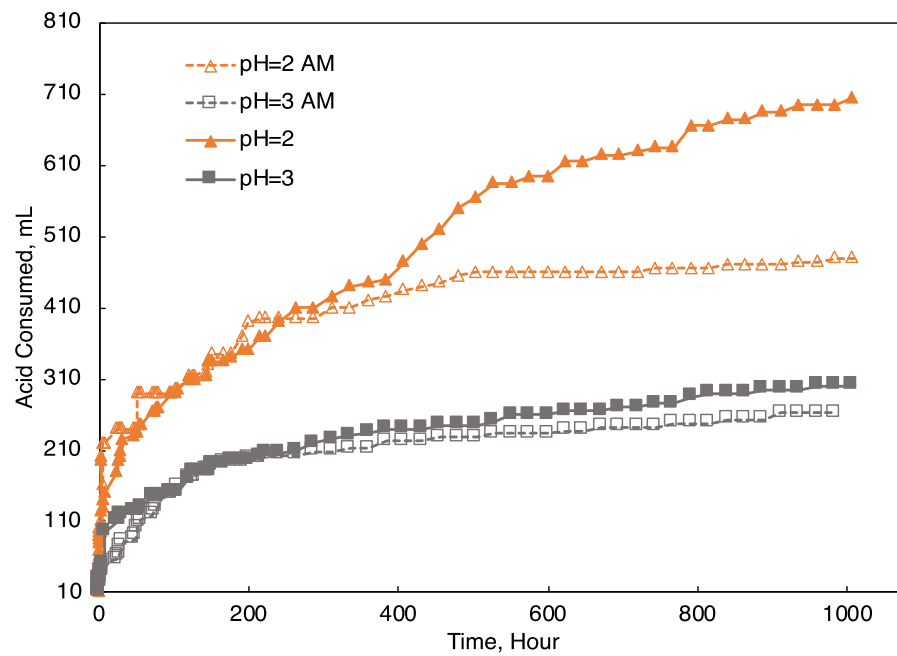
Figure-2.8: Sulfate concentrations in mg/L measured in specimen containers (a) with four different pHs for over 1000 hours or 42 days, and (b) in comparison of OPC and AM

2.3.4. Acid consumption

The acid consumption plot in Figure-2.9 reflects that of sulfate ion concentration in Figure-2.8. The container with the lowest pH consumed the highest amount of sulfuric acid and vice versa. From pH1 to pH4 cells, the total amount of acid being consumed was 1305, 705, 300, 270 mL respectively. The accelerated rate of acid consumption in the early period of the immersion supports the fact of calcium ions being leached at an increasing rate from fresh specimens and the equilibrium of sulfate and calcium reaction being reached eventually. Figure-2.9(b) compares the acid consumption of OPC and AM specimens, which reflects the plot in Figure-2.8(b), where the difference is significant in pH2 but not in pH3 containers.



(a)



(b)

Figure-2.9: a) acid consumption in the four different pH cells, b) acid consumption compared between OPC and AM specimens

2.3.5. Visual observation on the specimens and the exposure solutions

As shown in Figure-2.10, the precipitation started to be visually significant at around 7 days in every pH of the solutions and slowly grew thicker making the solutions cloudy as the experiment progressed. The precipitation was mostly collected around the specimens' surface. It was assumed to be calcium sulfate (CaSO_4) as efflorescence chemical reaction can occur by calcium hydroxide losing hydroxyl ions and sulfuric acid losing hydronium ions [35, 36]. Further chemical analysis is required to verify the precipitated product; however, this was not done as part of this study.



Figure-2.10: The precipitation in white color around the specimens in pH2 sulfuric acid solution after 14 days.

The pictures of the OPC specimens were taken before immersion, and after 21 and 42 days of immersion. The specimen's appearance was compared in Figure-2.11 and 2.12. After 21 days, the specimens from pH1 solution were observed to be the most severe in corrosion while the specimen from pH4 solution remained visually undamaged. The specimens in pH1 cell were completely deteriorated after about 27 days of immersion as shown in Figure-2.13. Therefore, the appearance comparison in 42 days was only made to the specimens in pH2, 3 and 4. White spots occurred around the specimen's surface from every pH of the solutions with the most concentrated in pH1. The specimen from pH4 solution

turned yellowish color in 21 days and a similar event happened to the specimen in pH3 solution in 42-days comparison.

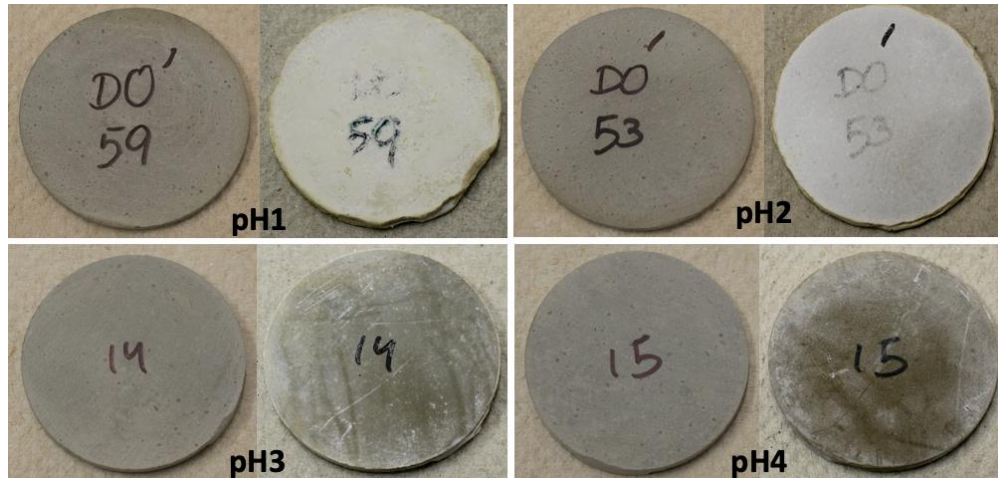


Figure-2.11: The appearance of specimens are compared before (left) and after (right) immersion of 21 days. The specimen in pH1 solution encountered the most severe corrosion while the specimen in pH4 solution remained visually undamaged.

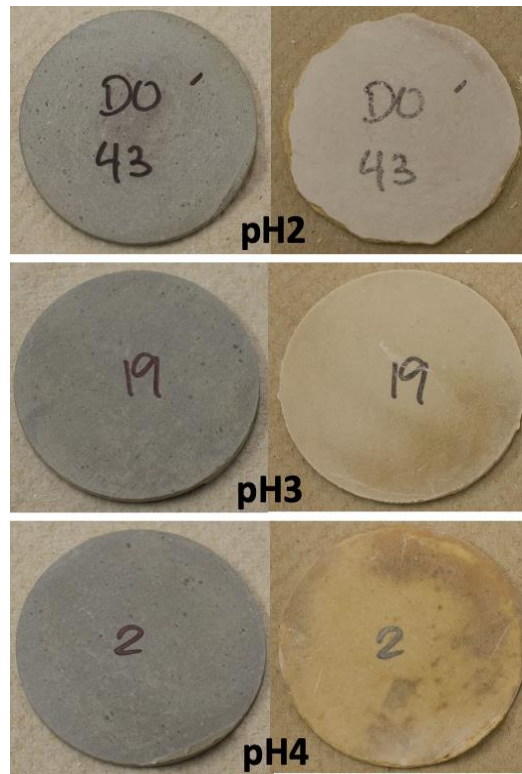


Figure-2.12: The appearance of specimens are compared before (left) and after (right) immersion of 42 days. The specimen from pH2 solution encountered the most severe corrosion (similar to pH1 at 21 days) while the specimen from pH3 and pH4 solution remained visually undamaged. The specimen in pH1 solution was completely deteriorated.

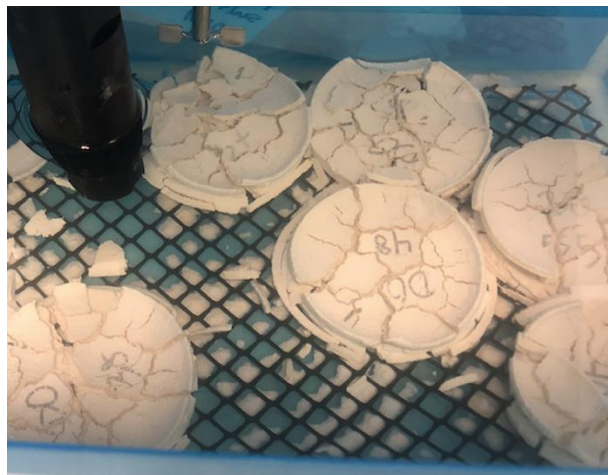


Figure-2.13: Specimens in pH1 solution were completely failed at around 27 days.

In addition to the pictures of the OPC specimens in four levels of pH, the pictures of AM specimens were also captured and compared against the OPC specimens in pH2 and pH3. Figure-2.14 compares the visual appearance of the AM specimens against the OPCs after 42 days of immersion. In pH2 solutions, the AM specimen was slightly damaged around the edge, but the damage in the OPC specimen appeared to be more severe. In pH3 solutions, the damage in both AM and OPC specimens was not visually recognized except the surface color of the AM specimen turned golden brown, which was possibly due to the topical treatment of the admixture. Additional study is required for further chemical analysis to explain the change of color, which is beyond the scope of this paper. However, the visual appearance in the AM specimens supports the fact that the effectiveness of the antimicrobial admixture becomes more significant in a more severe environment.

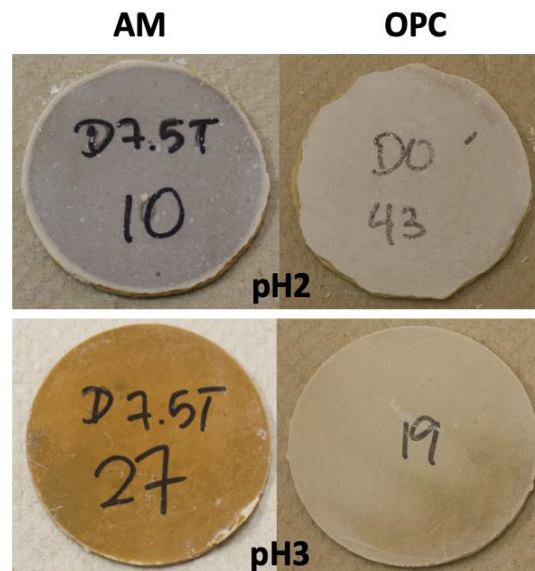


Figure-2.14: The AM specimens were compared against the OPC specimens after 42 days of immersion in pH2 and pH3 solutions

2.3.6. The B3B flexural strength test

The B3B test was performed after 21 and 42 days of immersion to observe the rate of strength reduction over time. Figure-2.15 shows the average specimens' strength being retained after a certain time of acid exposure. The OPC specimens from pH1 to pH4 cells

retained 43%, 79%, 90% and 96% respectively after 21 days of immersion. Given the increasing rate of deterioration, especially in pH1, the specimens in pH1 cell were completely failed around day 27 before the next test in 15 days while those in pH2 container retained 34% of strength after 42 days. The rate of deterioration was relatively slow in pH3 and pH4 cells remaining 84 and 91% of strength respectively after 42 days.

Figure-2.16 compares the AM specimens' strength against the OPC in pH2 and pH3 solutions. The effectiveness of antimicrobial admixture was significant after 42 days in pH2 solution and relatively visible in pH3 as well. In pH2 solutions, the AM specimens retained 77% of strength while the OPC specimens' strength was already reduced to 34% after 42 days. In pH3 solutions, the strength of AM and OPC specimens were retained at 84% and 80% respectively. This finding reinforces the result of Erbehtas et al. [13, 26] that concluded the antimicrobial admixture being effective in delaying MICC especially in lower pHs. The strength comparison between OPC and AM in Figure-2.16 also reflects the acid consumption plot in Figure-2.9(b), where the difference is significant in pH2 but not in pH3 containers.

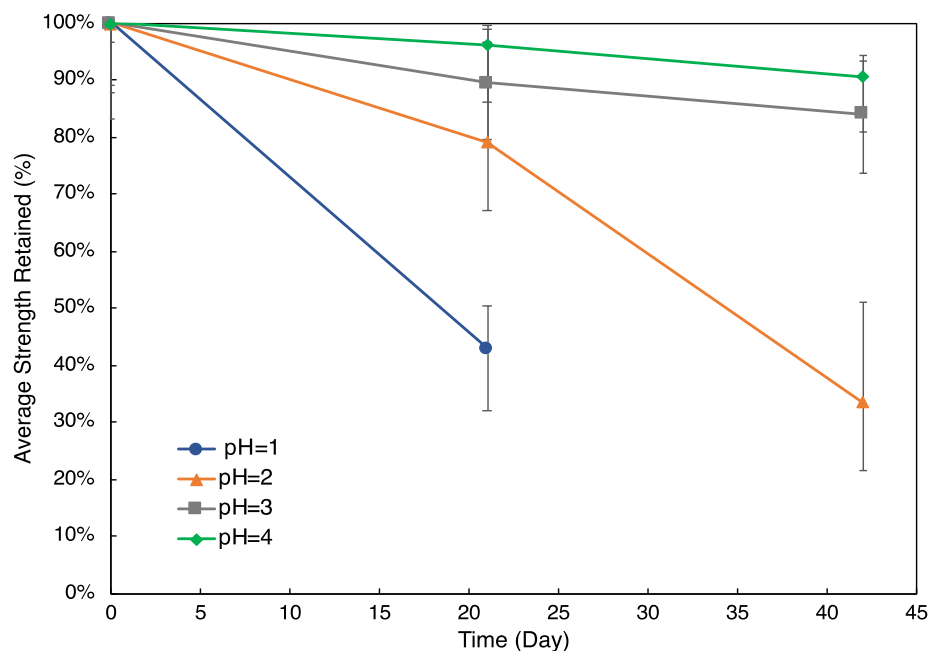


Figure-2.15: average retained flexural strength in percent (%) over 42 days of immersion: the specimens in pH1 cells were completely deteriorated around day 27 before the second test.

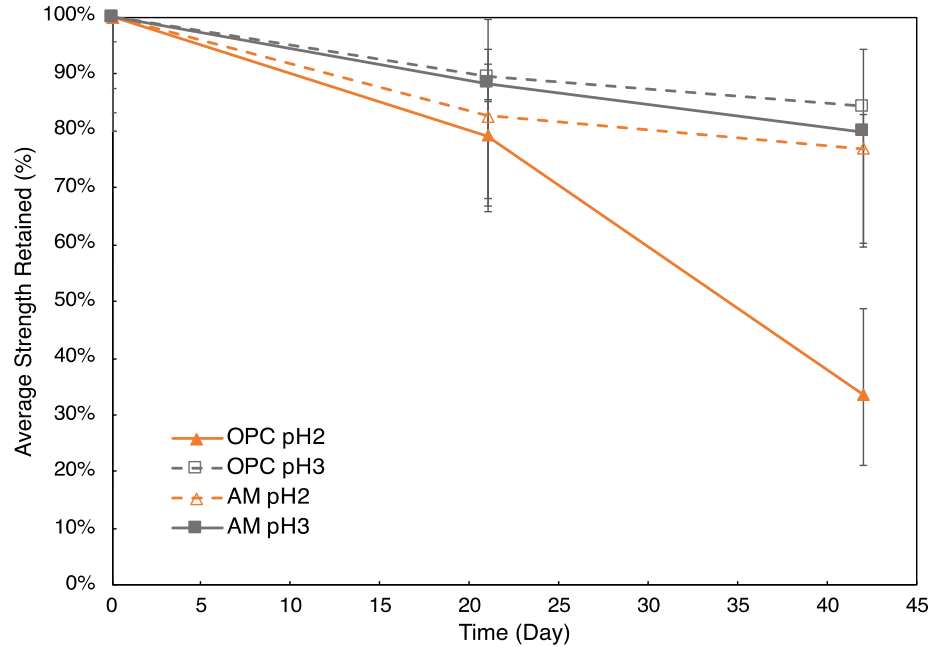


Figure-2.16: the retained flexural strength (%) of AM specimens compared against OPC in pH2 and pH3 solutions

2.4. Discussion

As the flexural strength of the specimens are related to the thickness of the specimens following Equation-2.2, the pH of the exposure solution was also correlated with the rate change of thickness over the first 21 days of exposure period. The relationship is shown in Figure-2.17 and quantified by:

$$c_r = 30.85e^{-0.813pH} \quad \text{Equation-2.6}$$

where c_r is the rate of change of thickness or corrosion rate of the paste specimens (mm/yr). The rates of thickness reduction per year from pH1 to pH4 solutions were 13.68 mm, 6.07 mm, 2.69 mm, and 1.19 mm, respectively.

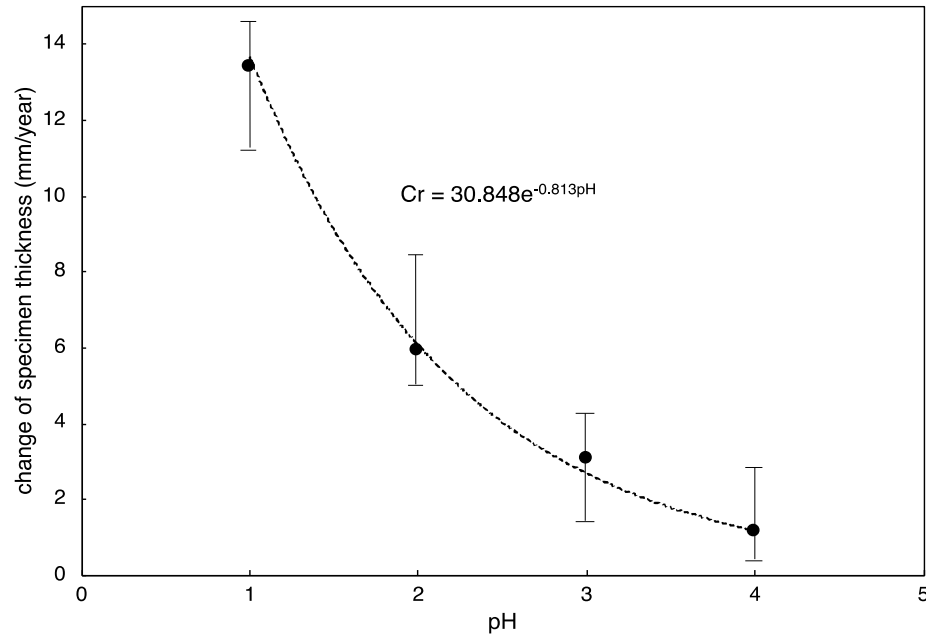


Figure-2.17: The rate of change of thickness, mm loss per year in terms of pH.

In the past, Pomeroy ^[22] developed a relationship for corrosion rate, c_r (mm/yr), and the H₂S exposure in sewer systems. This relationship, which is shown in Equation-2.7 has been used widely in the industry to predict corrosion rate of concrete exposed to H₂S-containing sewer environments.

$$c_r = 11.5k\phi_{sw} \frac{1}{A} \quad \text{Equation-2.7}$$

where k is a constant that depends on the climate (e.g., 0.8 for moderate climates), ϕ_{sw} is the available H₂S released and available on the surface of concrete g/(m²-h), and A is a measure of alkalinity of the cementitious system (e.g., paste, mortar, or concrete).

Equalizing Equations 2.6 and 2.7, after substituting known parameters, a moderate climate can be obtained:

$$c_r = 11.5 k \phi_{sw} \frac{1}{A} = 30.85e^{-0.813pH} \quad \text{Equation-2.8a}$$

$$\phi_{sw} = \frac{2.684e^{-0.813pH}}{k} \quad \text{Equation-2.8b}$$

which establishes a relationship between the chemical acid immersion test and the available H₂S concentration in a sewer system in a moderate climate. A similar relationship might also be developed between the biogenic acid immersion test; therefore, it is possible to relate all three tests to each other. This work is not within the scope of this study; however, it should be studied in the future.

2.5. Conclusion

A method of chemical acidification test that maintained the pH of the exposure media was developed. The method presented in this paper adopted the idea of automatically titrating the exposure solution by constantly monitoring its pH and having the system respond itself with minimum manual interference. The pH was observed to be more consistent in lower pH setpoints. A relative fluctuation was found in pH 3 and pH4.

In efforts to quantify the deterioration parameters, the amount of acid consumption in titrating exposure solutions, the amount of free calcium and sulfate ions, and the flexural strength reduction were recorded. Those parameters were plotted in terms of different pH levels against over time. However, since the acidification was maintained as a result of continuous sulfuric acid injection, the solution was always abundant in sulfate ions, which react with the leached calcium ions from the solution to form gypsum. Therefore, this paper suggests to use the acid consumption than the concentration of free calcium and sulfate ions to reflect the amount of leached calcium compounds, which provide the strength of the cementitious materials.

The flexural strength decreased significantly in the specimens from pH1 and pH2 sulfuric acid solutions while it was only slightly reduced in pH3 and pH4 solutions. The specimens in pH1 cells were completely failed approximately after 27 days of exposure. The rate of corrosion in every pH of the solutions was observed to be increasing as the experiment progressed, especially in pH1 and pH2. An empirical formula to calculate the rate of thickness reduction in terms of pH was developed. The thickness can be reduced from about 1mm to more than 10mm per year if cementitious materials was exposed to sulfuric acid solution with pH lower than pH4. It should be noted that this experiment only used cement paste specimens and further corrosion test on mortars and concrete was recommended. The relationship between the empirical formula in this chemical acidification test and the theoretical equation was established. The concentration of H₂S can be calculated by measuring the pH of the exposure media or sewer networks.

2.6. Acknowledgements

The authors would like to acknowledge the financial support from Concrete Sealants, Inc. for this research project.

2.7. References

1. *Standard Test Methods for Determining the Chemical Resistance of Concrete Products to Acid Attack*. 2020, ASTM C1898: ASTM International, West Conshohocken, PA.
2. *Standard Test Methods for Determination of the Effects of Biogenic Acidification on Concrete Antimicrobial Additives and/or Concrete Products*. 2020, ASTM C1904: ASTM International, West Conshohocken, PA.
3. Börger, A., P. Supancic, and R. Danzer, *The ball on three balls test for strength testing of brittle discs: stress distribution in the disc*. Journal of the European Ceramic Society, 2002. **22**(9): p. 1425-1436.
4. Börger, A., P. Supancic, and R. Danzer, *The ball on three balls test for strength testing of brittle discs: Part II: analysis of possible errors in the strength*

- determination. *Journal of the European Ceramic Society*, 2004. **24**(10): p. 2917-2928.
5. Cao, Y., et al., *The influence of cellulose nanocrystal additions on the performance of cement paste*. *Cement and Concrete Composites*, 2015. **56**: p. 73-83.
 6. Fu, T., et al., *The Influence of Cellulose Nanocrystals on the Hydration and Flexural Strength of Portland Cement Pastes*. *Polymers (Basel)*, 2017. **9**(9).
 7. Fu, T. and W. Weiss, *The Ball-on-Three-Ball (B3B) Test – Application to Cement Paste and Mortar*. *Advances in Civil Engineering Materials*, 2020. **9**(1): p. 128-142.
 8. Qiao, C., P. Suraneni, and J. Weiss, *Damage in cement pastes exposed to NaCl solutions*. *Construction and Building Materials*, 2018. **171**: p. 120-127.
 9. Qiao, C., P. Suraneni, and J. Weiss, *Flexural strength reduction of cement pastes exposed to CaCl₂ solutions*. *Cement and Concrete Composites*, 2018. **86**: p. 297-305.
 10. Cao, Y., et al., *Performance-enhanced cementitious materials by cellulose nanocrystal additions*. *Production and Applications of Cellulose Nanomaterials*, 2013. **2**.
 11. Cao, Y., et al., *The relationship between cellulose nanocrystal dispersion and strength*. *Construction and Building Materials*, 2016. **119**: p. 71-79.
 12. Erbehtas, A.R., O.B. Isgor, and W.J. Weiss, *Comparison of Chemical and Biogenic Acid Attack on Concrete*. *ACI Materials Journal*, 2020. **117**(1): p. 9.
 13. Erbehtas, A.R., O.B. Isgor, and W.J. Weiss, *An accelerated testing protocol for assessing microbially induced concrete deterioration during the bacterial attachment phase*. *Cement and Concrete Composites*, 2019. **104**: p. 103339.
 14. Hewayde, E., E.N. Allouche, and G.F. Nakhla, *Experimental Investigations of the Effect of Selected Admixtures on the Resistance of Concrete to Sulfuric Acid Attack*, in *New Pipeline Technologies, Security, and Safety*. 2003. p. 504-513.

15. Hewayde, E., et al., *Effect of Mixture Design Parameters and Wetting-Drying Cycles on Resistance of Concrete to Sulfuric Acid Attack*. Journal of Materials in Civil Engineering, 2007. **19**(2): p. 155-163.
16. Hewayde, E., et al., *Effect of geopolymer cement on microstructure, compressive strength and sulphuric acid resistance of concrete*. Magazine of Concrete Research, 2006. **58**(5): p. 321-331.
17. Hewayde, E., et al., *Using concrete admixtures for sulphuric acid resistance*. Proceedings of the Institution of Civil Engineers - Construction Materials, 2007. **160**(1): p. 25-35.
18. Monteny, J., et al., *Chemical and microbiological tests to simulate sulfuric acid corrosion of polymer-modified concrete*. Cement and Concrete Research, 2001. **31**(9): p. 1359-1365.
19. De Belie, N., et al., *Experimental research and prediction of the effect of chemical and biogenic sulfuric acid on different types of commercially produced concrete sewer pipes*. Cement and Concrete Research, 2004. **34**(12): p. 2223-2236.
20. House, M., et al., *Concrete Resistance to Sulfuric Acid Immersion: The Influence of Testing Details and Mixture Design on Performance as It Relates to Microbially Induced Corrosion*. Advances in Civil Engineering Materials, 2019. **8**(1): p. 544-557.
21. Pomeroy, R.D., *Pomeroy's Model of Corrosion Rate*. U.S. Environmental Protection Agency, 1974.
22. Pomeroy, R.D. and J.D. Parkhurst, *THE FORECASTING OF SULFIDE BUILD-UP RATES IN SEWERS*. 1978: Elsevier Ltd. 621-628.
23. Ding, L., *Assessing the performance of antimicrobial concrete admixtures in concrete subjected to microbially induced corrosion*. 2015: Purdue University.
24. *Standard Method of Test for Electrical Resistivity of a Concrete Cylinder Tested in a Uniaxial Resistance Test*. 2015, AASHTO TP119-15 (2019): AASHTO.
25. *Standard Specification for Portland Cement*. 2020, ASTM C150/C150M-20: ASTM International, West Conshohocken, PA.

26. Erbehtas, A.R., *Development of Practical Accelerated Testing Protocols for the Performance Evaluation of Concrete against Microbially Induced Corrosion of Concrete*. 2018, Oregon State University.
27. Qiu, L., et al., *Antimicrobial concrete for smart and durable infrastructures: A review*. *Construction and building materials*, 2020. **260**: p. 120456-120456.
28. Index, N.E.M., *Sulfate (Turbidimetric)*. 1978, EPA-NERL: 375.4: National Environmental Methods Index (NEMI).
29. Hulm, B.J., J.D. Parker, and W.J. Evans, *Biaxial strength of advanced materials*. *Journal of Materials Science*, 1998. **33**(13): p. 3255-3266.
30. Lee, J.H., et al., *Thermal shock behaviour of alumina ceramics by ball-on-3-ball test*. *Materials Letters*, 2002. **56**(6): p. 1022-1029.
31. Nohut, S., *A general formulation for strength prediction of advanced ceramics by ball-on-three-balls (B3B)-test with different multiaxial failure criteria*. *Ceramics International*, 2012. **38**(3): p. 2411-2420.
32. Shetty, D.K., et al., *A Biaxial-Flexure Test for Evaluating Ceramic Strengths*. *Journal of the American Ceramic Society*, 1983. **66**(1): p. 36-42.
33. Temenoff, J.S. and A.G. Mikos, *Biomaterials: the intersection of biology and materials science*. Vol. 1. 2008: Pearson/Prentice Hall Upper Saddle River, NJ, USA:.
34. House, M. *Using biological and physico-chemical test methods to assess the role of concrete mixture design in resistance to microbially induced corrosion*. 2013.
35. Mori, T., et al., *Interactions of nutrients, moisture and pH on microbial corrosion of concrete sewer pipes*. *Water Research*, 1992. **26**(1): p. 29-37.
36. Smith, G., *Calcite straw stalactites growing from concrete structures*. *Cave and Karst Science*, 2016. **43**(1): p. 4-10.
37. Björk, F. and C.A. Eriksson, *Measurement of alkalinity in concrete by a simple procedure, to investigate transport of alkaline material from the concrete slab to a self-levelling screed*. *Construction and Building Materials*, 2002. **16**(8): p. 535-542.

3. DETERMINING THE INFLUENCE OF SPECIMEN MIXING PROCEDURE AND DRYING TIME ON THE RESULTS OF THE B3B FLEXURAL STRENGTH TEST

3.1. Background and Motivation

It is widely known that cementitious materials have a higher compressive strength than tensile strength. The direct measurement of tensile strength is challenging^[1-3]. As a result, many test methods exist to obtain an indirect measure of the tensile strength, including the split tensile strength (ASTM C496)^[4] or flexural strength (ASTM C78, C293, C348)^[5-7]. The ball-on-three-ball (B3B) test method has been used to evaluate the strength of ceramic^[8-15], bone^[16], and cementitious materials^[17-27].

Traditionally, the compressive strength test (ASTM C39) the compressive strength test for chemical resistance of cementitious materials (ASTM C579), and the flexural strength tests using third-point (ASTM C78) or center point loading test (ASTM C293) are used to measure the mechanical properties of cement composites. Changes in strength, stiffness, and the stress to strain ratio can be obtained from these types of tests^[28-30] and used to assess changes over time or when exposed to different environments (e.g., acid degradation). As this damage generally occurs on the surface when tested in a severe environment and the surface damage is relatively small compared to the specimen size, this may require a relatively long time before the strength of the relatively large sample provides a measure of surface damage^[31, 32].

The B3B test uses thin-disk shaped specimens, which can be prepared to have several replicates by sectioning a concrete or cement paste cylinder. The increased number of samples improves the statistical reliability of the test. In addition, the high surface area of the B3B specimen geometry^[13, 34] enables strength change to be more easily detected^[19, 23, 26, 35].

While several test sample geometries have been used for B3B testing in the literature [4-6, 17, 27, 36-38], this paper will focus on the testing geometry illustrated in Figure-3.1, which is being used for cementitious samples like those in ASTM C1904-20^[17, 19, 23, 26, 35]. The device consists of three balls that provide base support and a central ball on the top used to provide loading. The disk-shaped specimen is placed on three balls positioned at 120° from each other under the specimen, as shown in Figure-3.1. Two positioning pins are used to center the specimen in the testing frame, as shown in Figure-3.1. After the specimen is centered, the positioning pins are carefully removed. The fourth ball is then loaded over the top at the center of the specimen. The loading head is initially moved at 2.5mm/min to bring the ball near contact with the sample, and the loading rate of 0.5mm/min is used from initial contact until the specimen fails. A load cell is used for the maximum load at failure (or the peak load). The thickness is measured at three points at the failure plane using a digital caliper with 0.01mm precision. The three measured thicknesses are averaged.

It should be noted that previous research identified that the strengths obtained from the B3B test could be higher than those obtained from more standard flexural beam tests^[17]. This is primarily related to 'size-effects' and the impact of Weibull effects and a strain gradient that develops in more conventional flexural testing^[31, 39]. It should be noted that the balls are permitted to rotate freely.

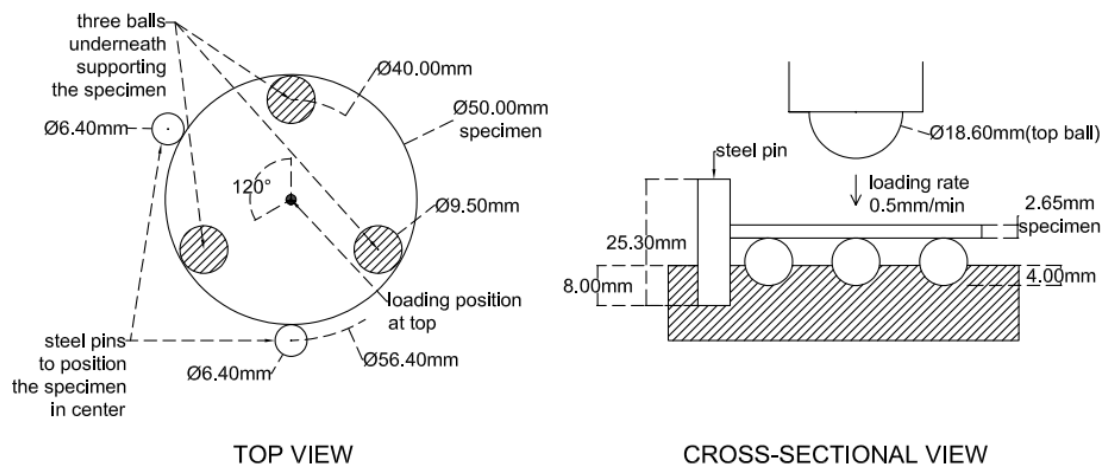


Figure-3.1: Ball-on-Three-Ball (B3B) Test Setup

The equation to interpret the results of the B3B test was developed by Börger et al.^[13, 14] and is shown in Equation-1.

$$\sigma = f(\alpha, \beta, \nu) \frac{F}{t^2} \quad \text{Equation-3.1}$$

where σ is the flexural strength, α and β are the geometry parameters, ν is the Poisson's ratio, F is the peak load, and t is the thickness of the specimen^[13, 14]. The geometry factors from Equation-1 are calculated using equations -2 through -4^[13, 14]:

$$f(\alpha, \beta, \nu) = C_0 + \frac{(C_1 + C_2\alpha + C_3\alpha^2 + C_4\alpha^3)(1 + C_6\beta)}{1 + C_5\alpha} \quad \text{Equation-3.2}$$

$$\alpha = \frac{t}{R} \quad \text{Equation-3.3}$$

$$\beta = \frac{R_a}{R} \quad \text{Equation-3.4}$$

To simplify this equation for use in ASTM C1904-20, it can be recognized that R_a and R are 20.6 mm and 25.4 mm, Poisson's ratio is 0.20 for cements. As a result, the six coefficients in $f(\alpha, \beta, \nu)$ are $C_0 = -12.354$, $C_1 = 15.549$, $C_2 = 489.2$, $C_3 = -78.707$, $C_4 = 52.216$, $C_5 = 36.554$, $C_6 = 0.082$ for the average R_a and R values. The geometry factor $f(\alpha, \beta, \nu)/t^2$ (i.e., all the terms other than the peak load F on the right side of equation 1) is plotted as a function of sample thickness Figure-3.2. Equation-5 provides an approximate measure of flexural strength as a function of thickness:

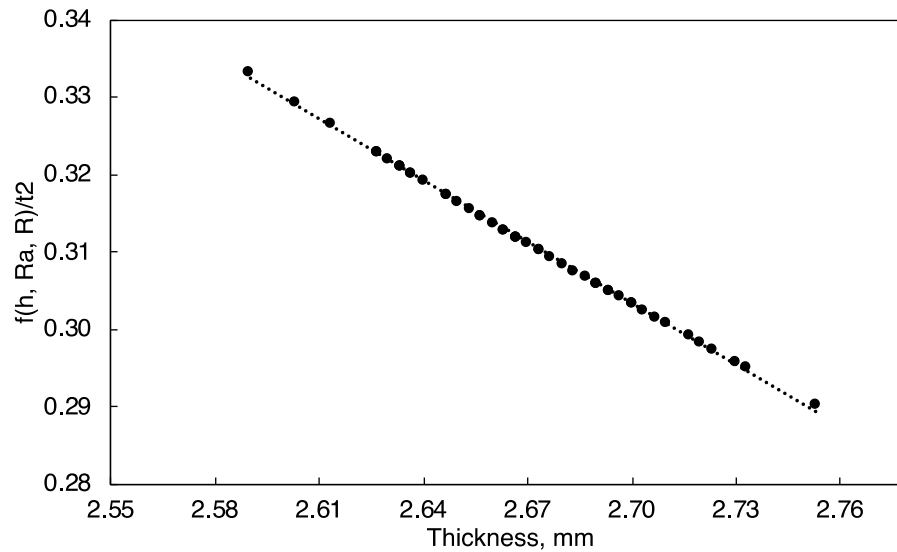
$$\sigma = (1.0145 - 0.2634t)F \quad \text{Equation-3.5}$$

where F (N) is the peak load, and t (mm) is the sample's thickness. The peak load and thickness can be obtained from measurements. It should be noted that the coefficients in Equation-5 can only be used with the peak load in units of Newton (N) and thickness in the units of millimeters (mm), resulting in a stress in units of megaPascals (MPa). The

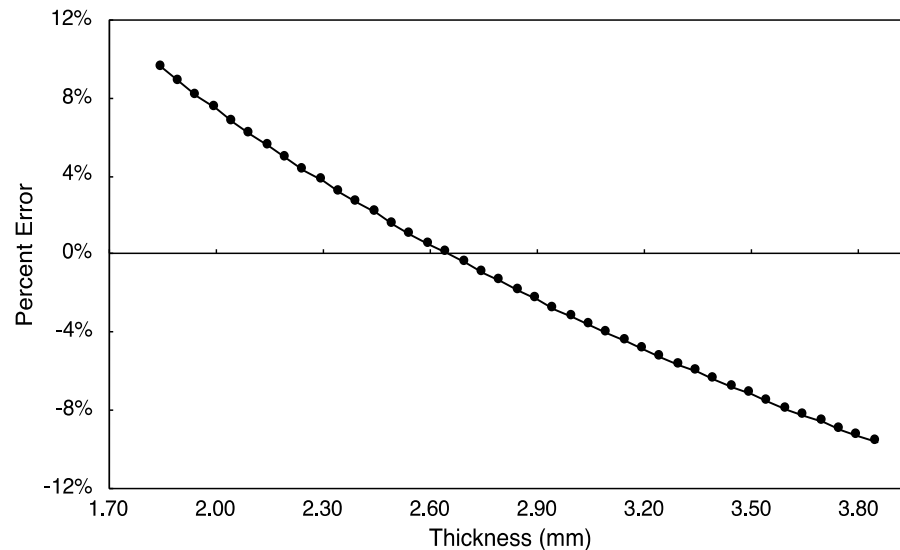
specimen's thickness beyond the range of 2.65 ± 0.20 mm will be non-linear, and the error of the linear approximation will increase. Equation 5 can further be simplified as equation-6 for specimens if the thickness is 2.65 mm.

$$\sigma = 0.315 F, (F \text{ in N, } s \text{ in MPa}) \quad \text{Equation-3.6}$$

Figure-3.2b shows the error for samples that comply with the ASTM C1904-20 specification thickness requirements.



(a)



(b)

Figure-3.2: Simplifications for the Calculation of Flexural Strength in the B3B test: a) $f(\alpha, \beta, v)/t^2$ plotted as a function of thickness b) error associated with the use of equation 6.

While Equation-6 appears suitable for simplification in ASTM C1904-20 if desired, the precise solution of Equation 1 is used for the remainder of this paper.

3.2. Objectives

ASTM C1904-20 provides a standard procedure to evaluate the performance of cementitious materials exposed to biogenic acidification. The standard uses a vacuum mixer in preparing test specimens. Although the vacuum mixer can avoid entrapped-air, the mechanical mixer specified in ASTM C305-20 is the more commonly used approach. Therefore, this paper investigated whether the use of different mixers influenced strength for both paste and mortar.

ASTM C1904-20 describes the use of the B3B test to evaluate the flexural strength of the specimens. A question has been raised about how long the specimens can be in air-drying conditions before testing them in the loading frame without affecting their strength. The second objective of this paper is to examine the influence of drying time on flexural strength.

3.3. Materials

Three types of mixtures are prepared in this study; cement paste, mortar-1, and mortar-2. The cement paste mixture was prepared with ordinary portland cement (OPC) (Type I/II) and deionized water (Type V). The mortar-1 mixture was prepared with OPC (Type I/II), deionized water (Type V), and graded silica sand, which complied with ASTM C778. The mortar-2 mixture was prepared with OPC (Type I/II), deionized water (Type V), and a local natural river sand. The water to cement ratio of all of the mixtures was 0.42. The cement had a Blaine fineness of 420 m²/kg. The oxide composition of the cement is given in Table-3.1. The fineness moduli for ASTM graded silica sand and river sand are 1.87 and 2.78, respectively. The ASTM graded sand's absorption capacity is approximately zero, while the river sand is 2.78%. The volumetric proportion of fine aggregate in both mortars is 50%. Mixture designs are shown in Table-3.2.

Table-3.1: Oxide Composition of the Type I/II ordinary portland cement (OPC) ASTM C150^[41] and AASHTO M85^[42]

Components	Mass (%)
Silicon dioxide (SiO ₂)	19.9
Aluminum oxide (Al ₂ O ₃)	4.6
Ferric oxide (Fe ₂ O ₃)	3.2
Calcium oxide (CaO)	62
Magnesium oxide (MgO)	3.8
Sulfur trioxide (SO ₃)	2.8
Loss on ignition (LOI)	1.6
Insoluble residue (IR)	0.7
Alkalies (Na ₂ O+0.658*K ₂ O)	0.57
Tricalcium silicate (C ₃ S)*	57
Dicalcium silicate (C ₂ S)*	14
Tricalcium aluminate (C ₃ A)*	7
Tetracalcium aluminoferrite (C ₄ AF)*	10
Limestone (CaCO ₃ – 86%)	1

*Cement chemistry notation: C = CaO, S = SiO₂, A = Al₂O₃, F = Fe₂O₃

Table-3.2: Mixture proportions used in this investigation (Mass in lb)

Mixture ID	Paste	Mortar-1 (Silica Sand)	Mortar-2 (River Sand)
Cement	84.61	42.31	42.31
Water	35.54	20.02	17.77
Fine Aggregate	-	81.05	82.68

3.4. Specimens Preparation Procedures

Two series of tests were performed in this experiment:

- (i) To determine the influence of the mixing types: vacuum mixer (ASTM C1904), mechanical mixing (ASTM C305), and high shear mixing (ASTM C1738).
- (ii) To determine the allowable time that a sample can be in air-dried condition after removal from the solution.

Vacuum mixing was performed using the Twister Evolution mixer (Renfert, St. Charles, IL) as described by 4^[17, 35, 40] and adopted in ASTM C1904 ^[43]. The vacuum mixer is used to reduce entrapped air in cement paste while mixing. The mixer was operated at a speed of 400 rpm under 80% vacuum for two 90 seconds periods. Between two mixing periods, the mixer bowl's inner surface and the blade were scrapped with a spatula for approximately 30 seconds to improve homogeneity. Conventional mixing (ASTM C305) was performed using a Hobart mixer (Hobart, Troy, OH). The standard procedure outlined in ASTM C305 was followed. ASTM C305 was used for both the pastes and the mortars. The high shear mixture was performed using a Waring blender (Waring Commercial, Stamford, CT). The standard procedures outlined in ASTM C1738 were followed for both the paste and the mortars.

Mixtures were prepared using each of the three methods mentioned above. After mixing, the samples were cast into cylindrical molds with a diameter of 50.8 ± 1.5 mm and a height of 101.6 ± 1.5 mm and sealed for 24 hours. The cylinders were rotated for 24 hours to minimize the potential for bleeding and segregation. The cylinders were cured for an additional 21 days under sealed conditions at temperature $23 \pm 2^\circ\text{C}$. After curing, the

cylinders were demolded and cut into disks with a 2.65 ± 0.25 mm thickness using a diamond blade wet saw (the samples are 50.8mm in diameter and 2.65 ± 0.25 mm in thickness). The top and bottom 20 mm of the cylinders were cut off and discarded, and only the central 60 mm portion was sliced into thin cylindrical specimens and used for testing. Each specimen's thickness was measured by using a digital caliper (Johnson, Mequon, WI). After cutting, the specimens were placed in limewater solution (i.e., calcium hydroxide solution with a concentration of 2g/L) in compliance with AASHTO TP119-15 (2017). The solution's volume was determined using a liquid volume (cm^3) to specimen surface area (cm^2) ratio of 4.67.

3.5. Data Acquisition Procedure

After 24 hours, the specimens were removed from the solution, gently patted with a paper towel to dry, and tested immediately for the standard flexural strength after patting dry. Table-3.3 shows the number of specimens that were tested for each mixer. To examine the influence of drying time, the samples were removed from the limewater. Some of the samples were tested wet, and some were tested after being allowed to dry for 1, 4, 9, 25, 64, and 121 minutes before the flexural strength testing began. The laboratory was at a standard temperature of $23 \pm 2^\circ\text{C}$ with an R.H. of $50 \pm 4\%$ R.H. Six specimens were tested at each drying period for statistical significance.

Table-3.3: Number of Thin-Disc Specimens Tested for Each Mixing Procedure and The Drying Test

Mixtures	Vacuum (ASTM C1904)	Hobart (ASTM C305)	Waring (ASTM 1738)
Paste	30	30	30
Mortar - 1	-	30	30
Mortar - 2	-	30	30
Paste (drying test)	Six at each drying age	-	-

ASTM E177-20 is often used as the method to determine standard deviation. ASTM E177-20 is more appropriate for large sample sizes; however, the method by Leys et al. [44] has more advantage for small sample size and is therefore used in this paper to determine outliers. After outliers were removed, statistical data analysis of flexural strengths was performed using the ANOVA (Analysis of Variance) method with a significance level of 0.05. Multiple groups were present in this experiment. If the result (p-value < 0.05) indicated a statistical difference at least in one group, the Tukey procedure (Honest Significant Difference)^[45, 46] was used to determine where a statistical difference occurred. The Tukey test was used since the sample sizes were different in each group. Equation-7 was used to calculate the critical range, or the smallest amount, the two means must vary from each other to be considered statically different. Therefore, if the absolute mean difference between the two groups of specimens is less than the critical range, those two groups are considered "not" statistically different, and vice versa^[45, 46].

$$Critical\ Range = Q \sqrt{\frac{MSW}{2} \left(\frac{1}{n_i} + \frac{1}{n_j} \right)} \quad \text{Equation-3.7}$$

where Q is the studentized range statistic (obtained from a standard q-table), MSW is the mean squared within groups, n_i is the number of observations in group "i," and n_j is the number of observations in group "j" ^[45, 46].

3.6. Data Analysis

3.6.1. Evaluation of the Impact of the Flexural Strength in Paste Made with Different Mixers

Figure-3.3 shows that the average flexural strength in cement paste specimens mixed with a vacuum mixer, a Hobart blender, and a Waring blender. The highest flexural strength occurred in the specimens made with the vacuum mixer, and the lowest strength was observed for the specimens made with the Waring blender. To determine the statistical difference between the specimens made with different mixers, an ANOVA test was

conducted. Table-3.4 shows the ANOVA test result. The probability of observing a result in ANOVA (i.e., the p-value) was 1×10^{-6} (< 0.05) and therefore indicated statistical difference with at least in at least one type series of samples made with one mixer. The Tukey test analysis was performed to determine which mixtures varied. No statistical difference in strengths was observed between the Vacuum and Hobart blender (Table-3.5); however, a significant difference was observed between the results of samples made in the Waring blender and samples made with either the Vacuum or Hobart mixers. Therefore, in cement paste specimens, the flexural strengths produced in the high-shear mixing method or Waring blender were statically different from the flexural strengths from the other two methods, vacuum and mechanical or Hobart blender. There was no statical difference between the vacuum mixer and Hobart blender when preparing paste specimens.

Similarly, the flexural strength of mortar-1 and mortar-2 prepared in the high-shear mixing or Waring blender is lower than that of samples mixed in the Hobart mixer (Figure-3.3). In Table-3.4, the p-values in both mortar-1 and mortar-2 are lower than the significance level of 0.05. The Tukey test in Table-3.5 shows statistical difference in mortar-1 specimens between high-shear mixing or Waring blender and mechanical mixing or Hobart blender. The Tukey test, as shown in Table-3.5, also suggests that mortar-2 specimens made with the rest of the mixers have a strength that is statically different between Waring and Hobart blenders.

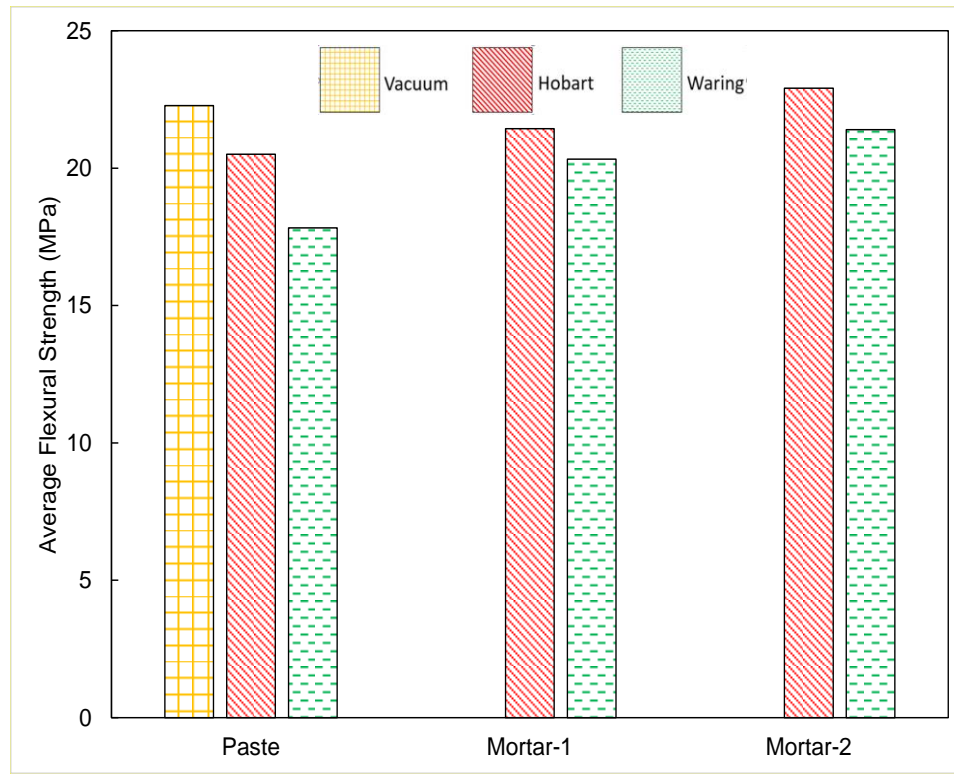


Figure-3.3: The average flexural strengths of cement paste and two mortars prepared by Vacuum, Hobart, and Waring blenders

Table-3.4: Summary of Statistics Collected from Paste and Mortars Specimens from Three Types of Mixers

Mixture	Mixer Type	Number of Tested Specimens	Average Flexural Strength, MPa	Standard Deviation, MPa	Coefficient of Variation, %	ANOVA p-value	Tukey Test Requirement
Paste	Vacuum	24	22.3	1.07	5%	0.0000026	Yes
	Hobart	27	20.5	2.15	11%		
	Waring	29	17.8	4.34	24%		
Mortar-1	Hobart	30	21.4	1.60	7%	0.0017	Yes
	Waring	30	20.3	0.92	5%		
Mortar-2	Hobart	26	22.9	1.31	6%	0.000054	Yes
	Waring	27	21.4	1.18	6%		

Table-3.5: Summary of the Tukey Significance Test Result on the Influence of Different Types of Mixers

Mixture	Pairs	Critical Range	Absolute Difference	Results
Paste	Vacuum/Hobart	1.985	1.769	Not Significant
	Vacuum/Waring	1.952	4.449	Significant
	Hobart/Waring	1.892	2.680	Significant
Mortar-1	Hobart/Waring	0.676	1.107	Significant
Mortar-2	Hobart/Waring	0.690	1.514	Significant

In addition to the influence of different mixing types, the same test data were used to investigate strength variation between paste and mortar specimens prepared within the same kind of mixer. The vacuum mixer was not used when mixing mortars, and therefore only the Hobart and Waring blenders were analyzed for strength variation between paste and mortars.

As shown in Table-3.7, when all three mixtures were prepared using Hobart blender, there is no statistical difference between paste and mortar-1 but mortar-2 is significantly different from the others. However, with the same type of mixing, the local river sand (mortar-2) has a higher strength than that of paste and mortar 1 (i.e., mortar with graded silica). Regardless of the mixing types, mortar with local river sand produces higher flexural strength than the cement paste.

Table-3.6: Summary of Statistics Collected from Paste and Mortars Specimens from Hobart and Waring Blenders

Mixer Type	Mixture	Number of Tested Specimens	Average Flexural Strength, MPa	Standard Deviation, MPa	Coefficient of Variation, %	ANOVA p-value	Tukey Test Requirement
Hobart	Paste	27	20.51	1.92	9%	0.000012	Yes
	Mortar-1	30	21.44	1.60	7%		
	Mortar-2	26	22.91	1.31	6%		
Waring	Paste	29	17.83	4.34	24%	0.000009	Yes
	Mortar-1	30	20.33	0.92	5%		
	Mortar-2	27	21.4	1.18	6%		

Table-3.7: Summary of Tukey Significance Test Result on the Strength Variation between Paste and Mortars

Mixer Type	Pairs	Critical Range	Absolute Difference	Results
Hobart	Paste/Mortar-1	1.091	0.933	Not Significant
	Paste/Mortar-2	1.131	2.404	Significant
	Mortar-1/Mortar-2	1.102	1.471	Significant
Waring	Paste/Mortar-1	1.091	2.505	Significant
	Paste/Mortar-2	1.131	3.570	Significant
	Mortar-1/Mortar-2	1.102	1.065	Not Significant

3.6.2. Evaluation of the Impact of the Flexural Strength in Paste Exposed to Differing Drying Time

As previously described, a series of samples were tested to determine the length of time a specimen could be exposed to drying during the testing process before the results were significantly impacted. Figure-3.4 shows the average flexural strengths as a function of drying time (the x-axis is the squared root of time). The error bars represent two standard deviations of the mean. It can be generally observed that initially, the mean strength stays relatively consistent with a similar variation. However, at later ages (i.e., 25 minutes, a square root drying time of 5 minutes), the average strength appears to decrease (from approximately 21 MPa to 16 MPa).

Figure-3.5 shows the coefficient of variation (COV) as a function of the square root of drying time. For shorter drying times (less than 10 minutes), the COV initially fluctuates below 6%; however, this increases at later ages (i.e., after 25 minutes).

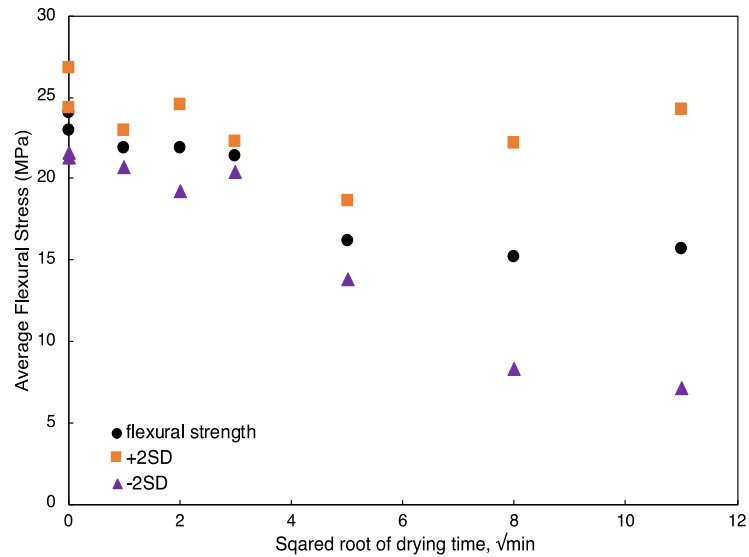


Figure-3.4: The flexural strength of paste samples as a function of drying time

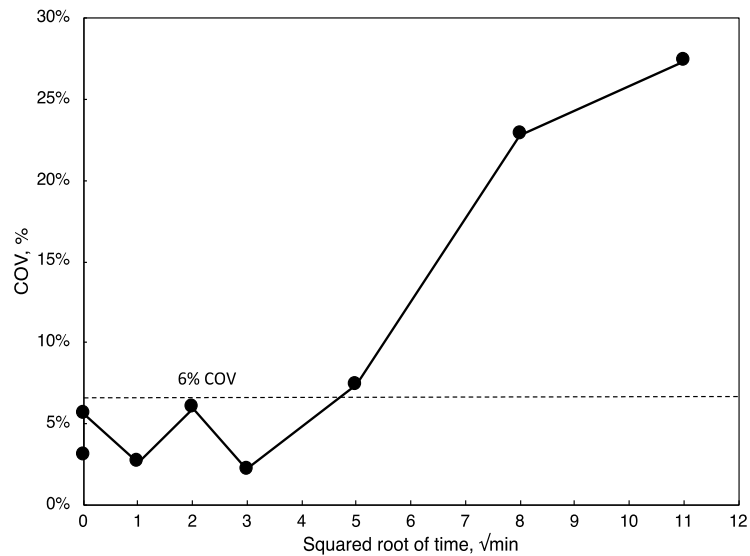


Figure-3.5: COV initially fluctuates below 6% and starts increasing at 25 minutes (a square root drying time of 5 square root minutes)

An ANOVA test was performed on the drying-time specimens' results, which resulted in a p-value of 1×10^{-9} , which was less than the significance level of 0.05 (Table-3.8), confirming a statistical difference of flexural strengths for at least in one group of drying-time test specimens. To determine the tests showing the difference, the Tukey test was applied. Table-3.9 provides a measure of the absolute mean difference between the two

groups. It can be observed that the absolute mean remains within the critical range for testing times of 0, 1, 4, and 9 minutes of drying time (i.e., the result is not significant). However, after drying for 25 minutes, the absolute mean is larger than the critical range, indicating a statistically significant strength (i.e., 25, 64, and 121 minutes). This shows that samples tested within 10 minutes (1 minute for testing and 9 minutes of drying) are statistically similar.

Table-3.8: Summary of Statistics Collected from Paste Specimens from Vacuum Blenders

Drying time, min	Number of Tested Specimens	Average Flexural Strength, MPa	Standard Deviation, MPa	Coefficient of Variation, %	Calculated Probability, p-value	Tukey Test Requirement
0 wet ¹	5	23.02	0.70	3%	0.000000009	Yes
0 dry ²	5	24.08	1.36	6%		
1	5	21.86	0.57	3%		
4	6	21.91	1.31	6%		
9	5	21.37	0.47	2%		
25	6	16.21	1.20	7%		
64	6	15.25	3.48	23%		
121	6	15.72	4.29	27%		

Note:

¹ Drying time when the specimen was removed from the solution and tested wet

² Drying time when the specimen was tested right after being patted dry with a paper towel

Table-3.9: Summary of Tukey Significance Test Result on the Influence of Drying Time

Pairs	Critical Range	Absolute Difference	Results
0 wet to 0 dry	3.809	1.065	Not Significant
0 wet to 1 min	3.809	1.156	Not Significant
0 wet to 4 min	3.647	1.105	Not Significant
0 wet to 9 min	3.809	1.649	Not Significant
0 wet to 25min	3.647	6.808	Significant
0 wet to 64 min	3.647	7.770	Significant
0 wet to 121 min	3.647	7.297	Significant

3.7. Conclusions

Three mixer types (Vacuum Mixer ASTM C1904, Hobart Mixer ASTM C 305, Waring Blender ASTM 1738) were used to prepare flexural strength of paste and mortar samples. This was done to determine whether different types of mixers can be used interchangeably. Based on the ANOVA and Tukey test results, the specimen's flexural strength (as determined from the B3B test) is statically the same for each mixer. The cement paste made using the Hobart blender would be interchangeable with paste specimens prepared with the vacuum mixer in ASTM C1904-20. As a result, there is ample evidence to permit this specification change. This allows ASTM C305-20 to be used with a more accessible mixer type for more laboratories.

The influence of the drying time on the flexural strength was examined. The result shows that the specimen's strength after drying for up to 9 minutes does not statistically vary from the strength of samples tested immediately after being removed from the solution or after pat dried. Therefore, the test should be performed approximately within 10 minutes after removing it from the solution. This appears to be a necessary addition for ASTM C1904-20 to aid in reducing variation.

3.8. Acknowledgments

The authors would like to acknowledge ASTM C13 committee for suggesting this study. The authors also acknowledge partial support for the graduate studies of the first author from of Concrete Sealants.

3.9. Reference

1. Popovics, S., *13 - Internal Structure of Concrete and Its Optimization*, in *Concrete Materials (Second Edition)*, S. Popovics, Editor. 1992, William Andrew Publishing: Oxford. p. 475-511.
2. MacGregor, J.G., et al., *Reinforced concrete: mechanics and design*. Vol. 3. 1997: Prentice Hall Upper Saddle River, NJ.

3. Mehta, P.K., *Concrete. Structure, properties and materials*. 1986.
4. *Standard Test Method for Splitting Tensile Strength of Cylindrical Concrete Specimens*. 2017, ASTM C496: ASTM International, West Conshohocken, PA.
5. *Standard Test Method for Flexural Strength of Concrete (Using Simple Beam with Third-Point Loading)*. 2018, ASTM C78: ASTM International, West Conshohocken, PA.
6. *Standard Test Method for Flexural Strength of Concrete (Using Simple Beam With Center-Point Loading)*. 2016, ASTM C293: ASTM International, West Conshohocken, PA.
7. *Standard Test Method for Flexural Strength of Hydraulic-Cement Mortars*. 2020, ASTM C348: ASTM International, West Conshohocken, PA.
8. Godfrey, D.J., *Fabrication, formulation, mechanical properties, and oxidation of sintered Si₃N₄ ceramics using disc specimens*. *Materials Science and Technology*, 1985. **1**(7): p. 510-515.
9. Hulm, B.J., J.D. Parker, and W.J. Evans, *Biaxial strength of advanced materials*. *Journal of Materials Science*, 1998. **33**(13): p. 3255-3266.
10. John B. Wachtman, W.R.C., M. John Matthewson, *Mechanical Properties of Ceramics*. 2nd ed. 2009, New York: Wiley. 496 Pages.
11. Munz, D., Fett, Theo, *Ceramics Mechanical Properties, Failure Behaviour, Materials Selection*. 1 ed. 1999: Springer-Verlag Berlin Heidelberg. X, 299.
12. Shetty, D.K., et al., *A Biaxial-Flexure Test for Evaluating Ceramic Strengths*. *Journal of the American Ceramic Society*, 1983. **66**(1): p. 36-42.
13. Börger, A., P. Supancic, and R. Danzer, *The ball on three balls test for strength testing of brittle discs: stress distribution in the disc*. *Journal of the European Ceramic Society*, 2002. **22**(9): p. 1425-1436.
14. Börger, A., P. Supancic, and R. Danzer, *The ball on three balls test for strength testing of brittle discs: Part II: analysis of possible errors in the strength determination*. *Journal of the European Ceramic Society*, 2004. **24**(10): p. 2917-2928.

15. Nohut, S., *A general formulation for strength prediction of advanced ceramics by ball-on-three-balls (B3B)-test with different multiaxial failure criteria*. *Ceramics International*, 2012. **38**(3): p. 2411-2420.
16. Temenoff, J.S. and A.G. Mikos, *Biomaterials: the intersection of biology and materials science*. Vol. 1. 2008: Pearson/Prentice Hall Upper Saddle River, NJ, USA:.
17. Fu, T. and W. Weiss, *The Ball-on-Three-Ball (B3B) Test – Application to Cement Paste and Mortar*. *Advances in Civil Engineering Materials*, 2020. **9**(1): p. 128-142.
18. Erbehtas, A.R., *Development of Practical Accelerated Testing Protocols for the Performance Evaluation of Concrete against Microbially Induced Corrosion of Concrete*. 2018, Oregon State University.
19. Erbehtas, A.R., O. Isgor, and W. Weiss, *Comparison of Chemical and Biogenic Acid Attack on Concrete*. *ACI Materials Journal*, 2020. **117**.
20. Cao, Y., et al., *The influence of cellulose nanocrystal additions on the performance of cement paste*. *Cement and Concrete Composites*, 2015. **56**: p. 73-83.
21. Cao, Y., et al., *The relationship between cellulose nanocrystal dispersion and strength*. *Construction and Building Materials*, 2016. **119**: p. 71-79.
22. Fu, T., et al., *The Influence of Cellulose Nanocrystals on the Hydration and Flexural Strength of Portland Cement Pastes*. *Polymers (Basel)*, 2017. **9**(9).
23. Qiao, C., P. Suraneni, and J. Weiss, *Flexural strength reduction of cement pastes exposed to CaCl₂ solutions*. *Cement and Concrete Composites*, 2018. **86**: p. 297-305.
24. Kim, J., C. Yi, and G. Zi, *Biaxial flexural strength of concrete by two different methods*. *Magazine of Concrete Research*, 2012. **64**: p. 1057-1065.
25. Cao, Y., et al., *Performance-enhanced cementitious materials by cellulose nanocrystal additions*. *Production and Applications of Cellulose Nanomaterials*, 2013. **2**.

26. Qiao, C., P. Suraneni, and J. Weiss, *Damage in cement pastes exposed to NaCl solutions*. Construction and Building Materials, 2018. **171**: p. 120-127.
27. *Standard Test Method for Flexural Toughness of Fiber Reinforced Concrete (Using Centrally Loaded Round Panel)*. 2020, ASTM C1550 - 20: ASTM International, West Conshohocken, PA.
28. *Standard Test Method for Compressive Strength of Cylindrical Concrete Specimens*. 2020, ASTM C39-20: ASTM International, West Conshohocken, PA.
29. *Standard Test Method for Flexural Strength of Concrete (Using Simple Beam with Third-Point Loading)*.
30. *Standard Test Method for Flexural Properties of Unreinforced and Reinforced Plastics and Electrical Insulating Materials by Four-Point Bending*. ASTM D6272-20: ASTM International, West Conshohocken, PA.
31. Konsta-Gdoutos, M.S., Z.S. Metaxa, and S.P. Shah, *Multi-scale mechanical and fracture characteristics and early-age strain capacity of high performance carbon nanotube/cement nanocomposites*. Cement and Concrete Composites, 2010. **32**(2): p. 110-115.
32. Konsta-Gdoutos, M.S., Z.S. Metaxa, and S.P. Shah, *Highly dispersed carbon nanotube reinforced cement based materials*. Cement and Concrete Research, 2010. **40**(7): p. 1052-1059.
33. House, M., et al., *Concrete Resistance to Sulfuric Acid Immersion: The Influence of Testing Details and Mixture Design on Performance as It Relates to Microbially Induced Corrosion*. Advances in Civil Engineering Materials, 2019. **8**(1): p. 544-557.
34. Wagemans, H., *Ball-on-ring test revisited*. Journal of the American Ceramic Society, 1989. **72**(8): p. 1538-1541.
35. Erbehtas, A.R., O.B. Isgor, and W.J. Weiss, *An accelerated testing protocol for assessing microbially induced concrete deterioration during the bacterial attachment phase*. Cement and Concrete Composites, 2019. **104**: p. 103339.

36. Dönmez, A. and Z.P. Bažant, *Size effect on punching strength of reinforced concrete slabs with and without shear reinforcement*. ACI Structural Journal, 2017. **114**(4): p. 875.
37. Fessler, H. and D.C.A. Fricker, *A Theoretical Analysis of the Ring-On-Ring Loading Disk Test*. Journal of the American Ceramic Society, 2006. **67**: p. 582-588.
38. Shetty, D., et al., *Biaxial Flexure Test for Ceramics*. Am. Ceram. Soc. Bull.; (United States), 1980. **59**:**12**.
39. Stamoulis, K. and A. Giannakopoulos, *Size effects on strength, toughness and fatigue crack growth of gradient elastic solids*. International Journal of Solids and Structures, 2008. **45**(18-19): p. 4921-4935.
40. Erbehtas, A.R., O.B. Isgor, and W.J. Weiss, *Comparison of Chemical and Biogenic Acid Attack on Concrete*. ACI Materials Journal, 2020. **117**(1): p. 9.
41. *Standard Specification for Portland Cement*. 2020, ASTM C150: ASTM International, West Conshohocken, PA.
42. *Standard Specification for Portland Cement*. 2020, AASHTO M85. p. 16.
43. *Standard Test Methods for Determination of the Effects of Biogenic Acidification on Concrete Antimicrobial Additives and/or Concrete Products*. 2020, ASTM C1904-20: ASTM International, West Conshohocken, PA.
44. Leys, C., et al., *Detecting outliers: Do not use standard deviation around the mean, use absolute deviation around the median*. Journal of Experimental Social Psychology, 2013. **49**(4): p. 764-766.
45. Conagin, A., D. Barbin, and C.G.B. Demétrio, *Modifications for the Tukey test procedure and evaluation of the power and efficiency of multiple comparison procedures*. Scientia Agricola, 2008. **65**(4): p. 428-432.
46. Driscoll, W.C., *Robustness of the ANOVA and Tukey-Kramer statistical tests*. Computers & Industrial Engineering, 1996. **31**(1-2): p. 265-268.

4. CONCLUSION

This first part of this thesis presents an automated chemical acidification test that keeps the pH of the exposure media consistent throughout time with minimal manual labor interference. The ball-on-three-ball flexural strength test was crucial in determining the rate of corrosion of cement paste specimens exposed to different levels of pH. The second part of the thesis addresses the questions typically encountered by many researchers when following ASTM C1898-20 and ASTM C1904-20. The influence of types of mixer and the influence of air-drying time over the strength of cement paste specimens were investigated. The conclusion from each chapter was drawn in the following sections.

4.1. Conclusion from Chapter-2

A method of chemical acidification test that maintained the pH of the exposure media was developed. The method presented in this paper adopted the idea of automatically titrating the exposure solution by constantly monitoring its pH and having the system respond itself with minimum manual interference. The pH was observed to be more consistent in lower pH setpoints. A relative fluctuation was found in pH 3 and pH4.

In efforts to quantify the deterioration parameters, the amount of acid consumption in titrating exposure solutions, the amount of free calcium and sulfate ions, and the flexural strength reduction were recorded. Those parameters were plotted in terms of different pH levels against over time. However, since the acidification was maintained as a result of continuous sulfuric acid injection, the solution was always abundant in sulfate ions, which react with the leached calcium ions from the solution to form gypsum. Therefore, this paper suggests to use the acid consumption than the concentration of free calcium and sulfate ions to reflect the amount of leached calcium compounds, which provide the strength of the cementitious materials.

The flexural strength decreased significantly in the specimens from pH1 and pH2 sulfuric acid solutions while it was only slightly reduced in pH3 and pH4 solutions. The specimens in pH1 cells were completely failed approximately after 27 days of exposure. The rate of corrosion in every pH of the solutions was observed to be increasing as the experiment progressed, especially in pH1 and pH2. An empirical formula to calculate the rate of thickness reduction in terms of pH was developed. The thickness can be reduced from about 1mm to more than 10mm per year if cementitious materials was exposed to sulfuric acid solution with pH lower than pH4. It should be noted that this experiment only used cement paste specimens and further corrosion test on mortars and concrete was recommended. The relationship between the empirical formula in this chemical acidification test and the theoretical equation was established. The concentration of H₂S can be calculated by measuring the pH of the exposure media or sewer networks.

4.2. Conclusion from Chapter-3

Three mixer types (Vacuum Mixer ASTM C1904, Hobart Mixer ASTM C 305, Waring Blender ASTM 1738) were used to prepare flexural strength of paste and mortar samples. This was done to determine whether different types of mixers can be used interchangeably. Based on the ANOVA and Tukey test results, the specimen's flexural strength (as determined from the B3B test) is statically the same for each mixer. The cement paste made using the Hobart blender would be interchangeable with paste specimens prepared with the vacuum mixer in ASTM C1904-20. As a result, there is ample evidence to permit this specification change. This allows ASTM C305-20 to be used with a more accessible mixer type for more laboratories.

The influence of the drying time on the flexural strength was examined. The result shows that the specimen's strength after drying for up to 9 minutes does not statistically vary from the strength of samples tested immediately after being removed from the solution or after pat dried. Therefore, the test should be performed approximately within 10 minutes after

removing it from the solution. This appears to be a necessary addition for ASTM C1904-20 to aid in reducing variation.

BIBLIOGRAPHY

1. (ASCE), A.S.o.C.E., *2017 Infrastructure Report Card: A Comprehensive Assessment of America's Infrastructure*. 2017: p. 112.
2. Alexander, M. and C. Fourie, *Performance of sewer pipe concrete mixtures with portland and calcium aluminate cements subject to mineral and biogenic acid attack*. *Materials and structures*, 2011. **44**(1): p. 313-330.
3. Ali Riza, E., O.B. Isgor, and W.J. Weiss, *Evaluating the efficacy of antimicrobial additives against biogenic acidification in simulated wastewater exposure solutions*. *RILEM Technical Letters*, 2019. **4**(0).
4. Allahverdi, A. and F. ŠKVÁRA, *Acidic corrosion of hydrated cement based materials*.
5. Bielefeldt, A., et al., *Bacterial kinetics of sulfur oxidizing bacteria and their biodeterioration rates of concrete sewer pipe samples*. *Journal of Environmental Engineering*, 2010. **136**(7): p. 731-738.
6. Börger, A., P. Supancic, and R. Danzer, *The ball on three balls test for strength testing of brittle discs: stress distribution in the disc*. *Journal of the European Ceramic Society*, 2002. **22**(9): p. 1425-1436.
7. Börger, A., P. Supancic, and R. Danzer, *The ball on three balls test for strength testing of brittle discs: Part II: analysis of possible errors in the strength determination*. *Journal of the European Ceramic Society*, 2004. **24**(10): p. 2917-2928.
8. Cao, Y., et al., *Performance-enhanced cementitious materials by cellulose nanocrystal additions*. *Production and Applications of Cellulose Nanomaterials*, 2013. **2**.
9. Cao, Y., et al., *The influence of cellulose nanocrystal additions on the performance of cement paste*. *Cement and Concrete Composites*, 2015. **56**: p. 73-83.
10. Cao, Y., et al., *The relationship between cellulose nanocrystal dispersion and strength*. *Construction and Building Materials*, 2016. **119**: p. 71-79.
11. *Ceramics– Silikáty*, 2000. **44**(4): p. 152-160.

12. Carde, C., R. François, and J.-M. Torrenti, *Leaching of both calcium hydroxide and C-S-H from cement paste: Modeling the mechanical behavior*. Cement and Concrete Research, 1996. **26**(8): p. 1257-1268.
13. Conagin, A., D. Barbin, and C.G.B. Demétrio, *Modifications for the Tukey test procedure and evaluation of the power and efficiency of multiple comparison procedures*. Scientia Agricola, 2008. **65**(4): p. 428-432.
14. De Belie, N., et al., *Experimental research and prediction of the effect of chemical and biogenic sulfuric acid on different types of commercially produced concrete sewer pipes*. Cement and Concrete Research, 2004. **34**(12): p. 2223-2236.
15. Ding, L., *Assessing the performance of antimicrobial concrete admixtures in concrete subjected to microbially induced corrosion*. 2015: Purdue University.
16. Ding, L., W.J. Weiss, and E.R. Blatchley, *Effects of Concrete Composition on Resistance to Microbially Induced Corrosion*. Journal of Environmental Engineering, 2017. **143**(6): p. 04017014.
17. Dönmez, A. and Z.P. Bažant, *Size effect on punching strength of reinforced concrete slabs with and without shear reinforcement*. ACI Structural Journal, 2017. **114**(4): p. 875.
18. Driscoll, W.C., *Robustness of the ANOVA and Tukey-Kramer statistical tests*. Computers & Industrial Engineering, 1996. **31**(1-2): p. 265-268.
19. Droste, R.L. and R.L. Gehr, *Theory and practice of water and wastewater treatment*. 2018: John Wiley & Sons.
20. Ehrich, S., et al., *Biogenic and Chemical Sulfuric Acid Corrosion of Mortars*. Journal of Materials in Civil Engineering, 1999. **11**(4): p. 340-344.
21. Emmanuel, K.A. and H.R. Sami, *Response of Concrete to Sulfuric Acid Attack*. ACI Materials Journal. **85**(6).
22. Erbehtas, A.R., *Development of Practical Accelerated Testing Protocols for the Performance Evaluation of Concrete against Microbially Induced Corrosion of Concrete*. 2018, Oregon State University.

23. Erbehtas, A.R., O.B. Isgor, and W.J. Weiss, *An accelerated testing protocol for assessing microbially induced concrete deterioration during the bacterial attachment phase*. Cement and Concrete Composites, 2019. **104**: p. 103339.
24. Erbehtas, A.R., O. Isgor, and W. Weiss, *Comparison of Chemical and Biogenic Acid Attack on Concrete*. ACI Materials Journal, 2020. **117**.
25. Fessler, H. and D.C.A. Fricker, *A Theoretical Analysis of the Ring-On-Ring Loading Disk Test*. Journal of the American Ceramic Society, 2006. **67**: p. 582-588.
26. Fu, T. and W. Weiss, *The Ball-on-Three-Ball (B3B) Test – Application to Cement Paste and Mortar*. Advances in Civil Engineering Materials, 2020. **9**(1): p. 128-142.
27. Fu, T., et al., *The Influence of Cellulose Nanocrystals on the Hydration and Flexural Strength of Portland Cement Pastes*. Polymers (Basel), 2017. **9**(9).
28. Ling, A.L., et al., *High-Resolution Microbial Community Succession of Microbially Induced Concrete Corrosion in Working Sanitary Manholes*. PLOS ONE, 2015. **10**(3): p. e0116400.
29. Gabrisova, A., J. Havlica, and S. Sahu, *Stability of calcium sulphoaluminate hydrates in water solutions with various pH values*. Cement and Concrete Research, 1991. **21**(6): p. 1023-1027.
30. Godfrey, D.J., *Fabrication, formulation, mechanical properties, and oxidation of sintered Si₃N₄ ceramics using disc specimens*. Materials Science and Technology, 1985. **1**(7): p. 510-515.
31. Grengg, C., et al., *Microbiologically induced concrete corrosion: A case study from a combined sewer network*. Cement and Concrete Research, 2015. **77**: p. 16-25.
32. Gutberlet, T., H. Hilbig, and R. Beddoe, *Acid attack on hydrated cement—Effect of mineral acids on the degradation process*. Cement and Concrete Research, 2015. **74**: p. 35-43.
33. Gutiérrez-Padilla, M.G.D., et al., *Biogenic sulfuric acid attack on different types of commercially produced concrete sewer pipes*. Cement and Concrete Research, 2010. **40**(2): p. 293-301.

34. Hewayde, E., et al., *Using concrete admixtures for sulphuric acid resistance*. Proceedings of the Institution of Civil Engineers - Construction Materials, 2007. **160**(1): p. 25-35.
35. Hewayde, E., et al., *Effect of Mixture Design Parameters and Wetting-Drying Cycles on Resistance of Concrete to Sulfuric Acid Attack*. Journal of Materials in Civil Engineering, 2007. **19**(2): p. 155-163.
36. House, M., et al., *Concrete Resistance to Sulfuric Acid Immersion: The Influence of Testing Details and Mixture Design on Performance as It Relates to Microbially Induced Corrosion*. Advances in Civil Engineering Materials, 2019. **8**(1): p. 544-557.
37. Huber, B., et al., *Characterization of sulfur oxidizing bacteria related to biogenic sulfuric acid corrosion in sludge digesters*. BMC Microbiology, 2016. **16**(1): p. 153.
38. House, M. *Using biological and physico-chemical test methods to assess the role of concrete mixture design in resistance to microbially induced corrosion*. 2013.
39. House, M., Weiss, J., *Review of Microbially Induced Corrosion and Comments on Needs Related to Testing Procedures*. Proceedings of the 4th International Conference on the Durability of Concrete Structures, 2014.
40. Huber, B., et al., *Evaluation of concrete corrosion after short- and long-term exposure to chemically and microbially generated sulfuric acid*. Cement and Concrete Research, 2017. **94**: p. 36-48.
41. Huber, B., et al., *Comparative analysis of biogenic and chemical sulfuric acid attack on hardened cement paste using laser ablation-ICP-MS*. Cement and Concrete Research, 2016. **87**: p. 14-21.
42. Hulm, B.J., J.D. Parker, and W.J. Evans, *Biaxial strength of advanced materials*. Journal of Materials Science, 1998. **33**(13): p. 3255-3266.
43. Islander, R.L., et al., *Microbial Ecology of Crown Corrosion in Sewers*. Journal of Environmental Engineering, 1991. **117**: p. 751-770.
44. John B. Wachtman, W.R.C., M. John Matthewson, *Mechanical Properties of Ceramics*. 2nd ed. 2009, New York: Wiley. 496 Pages.

45. Joseph, A.P., et al., *Surface neutralization and H₂S oxidation at early stages of sewer corrosion: influence of temperature, relative humidity and H₂S concentration*. Water research, 2012. **46**(13): p. 4235-4245.
46. Kim, J., C. Yi, and G. Zi, *Biaxial flexural strength of concrete by two different methods*. Magazine of Concrete Research, 2012. **64**: p. 1057-1065.
47. Konsta-Gdoutos, M.S., Z.S. Metaxa, and S.P. Shah, *Multi-scale mechanical and fracture characteristics and early-age strain capacity of high performance carbon nanotube/cement nanocomposites*. Cement and Concrete Composites, 2010. **32**(2): p. 110-115.
48. Konsta-Gdoutos, M.S., Z.S. Metaxa, and S.P. Shah, *Highly dispersed carbon nanotube reinforced cement based materials*. Cement and Concrete Research, 2010. **40**(7): p. 1052-1059.
49. Li, X., et al., *The Ecology of Acidophilic Microorganisms in the Corroding Concrete Sewer Environment*. Frontiers in Microbiology, 2017. **8**(683).
50. Larreur-Cayol, S., A. Bertron, and G. Escadeillas, *Degradation of cement-based materials by various organic acids in agro-industrial waste-waters*. Cement and Concrete Research, 2011. **41**(8): p. 882-892.
51. Leys, C., et al., *Detecting outliers: Do not use standard deviation around the mean, use absolute deviation around the median*. Journal of Experimental Social Psychology, 2013. **49**(4): p. 764-766.
52. Matthieu, P.L., et al., *Innovative approach to simulating the biodeterioration of industrial cementitious products in sewer environment. Part II: Validation on CAC and BFSC linings*. Cement and Concrete Research, 2016. **79**.
53. MacGregor, J.G., et al., *Reinforced concrete: mechanics and design*. Vol. 3. 1997: Prentice Hall Upper Saddle River, NJ.
54. Mehta, P.K., *Concrete. Structure, properties and materials*. 1986.
55. Mehta, P.K. and P.J. Monteiro, *Concrete: microstructure, properties, and materials*. 2014: McGraw-Hill Education.

56. Metcalf, et al., *Wastewater Engineering: Treatment and Reuse*. 2002: McGraw-Hill Education.
57. Monteny, J., et al., *Chemical and microbiological tests to simulate sulfuric acid corrosion of polymer-modified concrete*. *Cement and Concrete Research*, 2001. **31**(9): p. 1359-1365.
58. Monteny, J., et al., *Chemical, microbiological, and in situ test methods for biogenic sulfuric acid corrosion of concrete*. *Cement and Concrete Research*, 2000. **30**(4): p. 623-634.
59. Mori, T., et al., *Interactions of nutrients, moisture and pH on microbial corrosion of concrete sewer pipes*. *Water Research*, 1992. **26**(1): p. 29-37.
60. Mori, T., et al., *Microbial Corrosion of Concrete Sewer Pipes, H₂S Production from Sediments and Determination of Corrosion Rate*. *Water Science and Technology*, 1991. **23**(7-9): p. 1275-1282.
61. Munz, D., Fett, Theo, *Ceramics Mechanical Properties, Failure Behaviour, Materials Selection*. 1 ed. 1999: Springer-Verlag Berlin Heidelberg. X, 299.
62. *New ASTM Standard Test Methods for Determining the Chemical Resistnace of Concrete Products to Acid Attack*. 2020, ASTM International: West Conshohocken, PA.
63. Nica, D., et al., *Isolation and characterization of microorganisms involved in the biodeterioration of concrete in sewers*. *International biodeterioration & biodegradation*, 2000. **46**(1): p. 61-68.
64. Nohut, S., *A general formulation for strength prediction of advanced ceramics by ball-on-three-balls (B3B)-test with different multiaxial failure criteria*. *Ceramics International*, 2012. **38**(3): p. 2411-2420.
65. Okabe, S., et al., *Succession of Sulfur-Oxidizing Bacteria in the Microbial Community on Corroding Concrete in Sewer Systems*. *Applied and Environmental Microbiology*, 2007. **73**(3): p. 971.
66. Parker, C.D., *Mechanics of Corrosion of Concrete Sewers by Hydrogen Sulfide*. *Sewage and Industrial Wastes*, 1951. **23**(12): p. 1477-1485.

67. Parker, C.D., *Species of Sulphur Bacteria Associated with the Corrosion of Concrete*. Nature, 1947. **159**(4039): p. 439-440.
68. Parker, C.D., *THE CORROSION OF CONCRETE*. Australian Journal of Experimental Biology and Medical Science, 1945. **23**(2): p. 91-98.
69. Padival, N.A., J.S. Weiss, and R.G. Arnold, *Control of Thiobacillus by Means of Microbial Competition: Implications for Corrosion of Concrete Sewers*. Water Environment Research, 1995. **67**(2): p. 201-205.
70. Peyre Lavigne, M., et al., *An innovative approach to reproduce the biodeterioration of industrial cementitious products in a sewer environment. Part I: Test design*. Cement and Concrete Research, 2015. **73**: p. 246-256.
71. Pomeroy, R.D. and J.D. Parkhurst, *THE FORECASTING OF SULFIDE BUILD-UP RATES IN SEWERS*. 1978: Elsevier Ltd. 621-628.
72. Pomeroy, R.D., *Pomeroy's Model of Corrosion Rate*. U.S. Environmental Protection Agency, 1974.
73. Popovics, S., *13 - Internal Structure of Concrete and Its Optimization*, in *Concrete Materials (Second Edition)*, S. Popovics, Editor. 1992, William Andrew Publishing: Oxford. p. 475-511.
74. Qiao, C., P. Suraneni, and J. Weiss, *Damage in cement pastes exposed to NaCl solutions*. Construction and Building Materials, 2018. **171**: p. 120-127.
75. Qiao, C., P. Suraneni, and J. Weiss, *Flexural strength reduction of cement pastes exposed to CaCl₂ solutions*. Cement and Concrete Composites, 2018. **86**: p. 297-305.
76. Reardon, E., *An ion interaction model for the determination of chemical equilibria in cement/water systems*. Cement and Concrete Research, 1990. **20**(2): p. 175-192.
77. Roberts, D., et al., *Quantifying microbially induced deterioration of concrete: initial studies*. International Biodeterioration & Biodegradation, 2002. **49**(4): p. 227-234.
78. Sand, W. and E. Bock, *Concrete corrosion in the Hamburg Sewer system*. Environmental Technology Letters, 1984. **5**(12): p. 517-528.
79. Sand, W., E. Bock, and D. White. *Biotest system for rapid evaluation of concrete resistance to sulfur-oxidizing bacteria*. 1987.

80. Santo Domingo, J.W., et al., *Molecular survey of concrete sewer biofilm microbial communities*. Biofouling, 2011. **27**(9): p. 993-1001.
81. Saricimen, H., et al., *Durability of proprietary cementitious materials for use in wastewater transport systems*. Cement and Concrete Composites, 2003. **25**(4): p. 421-427.
82. Shetty, D.K., et al., *A Biaxial-Flexure Test for Evaluating Ceramic Strengths*. Journal of the American Ceramic Society, 1983. **66**(1): p. 36-42.
83. Shetty, D., et al., *Biaxial Flexure Test for Ceramics*. Am. Ceram. Soc. Bull.; (United States), 1980. **59**:12.
84. Soleimani, S., O.B. Isgor, and B. Ormeci, *Effectiveness of *E. coli* Biofilm on Mortar to Inhibit Biodegradation by Biogenic Acidification*. Journal of Materials in Civil Engineering, 2016. **28**(4): p. 04015167.
85. Soleimani, S., O. Isgor, and B. Ormeci, *Resistance of biofilm-covered mortars to microbiologically influenced deterioration simulated by sulfuric acid exposure*. Cement and Concrete Research, 2013. **53**: p. 229-238.
86. Stamoulis, K. and A. Giannakopoulos, *Size effects on strength, toughness and fatigue crack growth of gradient elastic solids*. International Journal of Solids and Structures, 2008. **45**(18-19): p. 4921-4935.
87. *Standard Guide for Microbially Induced Corrosion of Concrete Products*. 2019, ASTM C1894-19: ASTM International, West Conshohocken, PA.
88. *Standard Test Methods for Chemical Resistance of Mortars, Grouts, and Monolithic Surfacing and Polymer Concretes*. 2020, ASTM C267: ASTM International, West Conshohocken, PA.
89. *Standard Test Method for Compressive Strength of Cylindrical Concrete Specimens*. 2020, ASTM C39-20: ASTM International, West Conshohocken, PA.
90. *Standard Test Methods for Determination of the Effects of Biogenic Acidification on Concrete Antimicrobial Additives and/or Concrete Products*. 2020, ASTM C1904: ASTM International, West Conshohocken, PA.

91. *Standard Test Method for Flexural Strength of Concrete (Using Simple Beam With Center-Point Loading)*. 2016, ASTM C293: ASTM International, West Conshohocken, PA.
92. *Standard Test Method for Flexural Strength of Concrete (Using Simple Beam with Third-Point Loading)*. 2018, ASTM C78: ASTM International, West Conshohocken, PA.
93. *Standard Test Method for Flexural Strength of Hydraulic-Cement Mortars*. 2020, ASTM C348: ASTM International, West Conshohocken, PA.
94. *Standard Test Method for Flexural Properties of Unreinforced and Reinforced Plastics and Electrical Insulating Materials by Four-Point Bending*. ASTM D6272-20: ASTM International, West Conshohocken, PA.
95. *Standard Specification for Portland Cement*. 2020, AASHTO M85. p. 16.
96. *Standard Specification for Portland Cement*. 2020, ASTM C150: ASTM International, West Conshohocken, PA.
97. *Standard Test Method for Splitting Tensile Strength of Cylindrical Concrete Specimens*. 2017, ASTM C496: ASTM International, West Conshohocken, PA.
98. *Standard Test Method for Flexural Toughness of Fiber Reinforced Concrete (Using Centrally Loaded Round Panel)*. 2020, ASTM C1550 - 20: ASTM International, West Conshohocken, PA.
99. Sydney, R., E. Esfandi, and S. Surapaneni, *Control Concrete Sewer Corrosion via the Crown Spray Process*. Water Environment Research, 1996. **68**(3): p. 338-347.
100. Temenoff, J.S. and A.G. Mikos, *Biomaterials: the intersection of biology and materials science*. Vol. 1. 2008: Pearson/Prentice Hall Upper Saddle River, NJ, USA.
101. Vincke, E., et al., *A new test procedure for biogenic sulfuric acid corrosion of concrete*. Biodegradation, 1999. **10**(6): p. 421-428.
102. Wagemans, H., *Ball-on-ring test revisited*. Journal of the American Ceramic Society, 1989. **72**(8): p. 1538-1541.
103. Warren, C. and E. Reardon, *The solubility of ettringite at 25 C*. Cement and Concrete Research, 1994. **24**(8): p. 1515-1524.

104. Wu, L., C. Hu, and W.V. Liu, *The Sustainability of Concrete in Sewer Tunnel—A Narrative Review of Acid Corrosion in the City of Edmonton, Canada*. *Sustainability*, 2018. **10**(2): p. 517.
105. Yousefi, A., A. Allahverdi, and P. Hejazi, *Accelerated biodegradation of cured cement paste by Thiobacillus species under simulation condition*. *International Biodeterioration & Biodegradation*, 2014. **86**: p. 317-326.

APPENDIX - PRELIMINARY AND EXPLORATORY STUDIES TO STABILIZE THE PH IN CHEMICAL ACIDIFICATION TESTS

A.1. Background

One of the most challenging tasks in chemical acid immersion tests for cementitious materials is to keep the pH of the exposure solution at constant and stable, which is challenging due to leaching from the deteriorated cementitious matrix. The developed automatic acid immersion test presented in Chapter 2 solves this issue. However, before the development of the automated approach, preliminary and exploratory studies were performed to investigate different approaches to maintain the pH of the exposure solution stable. These studies are presented in this Appendix.

A.2. Objectives

Different amounts of sulfuric acid solution were used for chemical acidification test in the past literature. House et al.^[1] used solution to sample volume ratio 4.2 to 1, which was also presented in ASTM C1898^[2]. However, some research suggested to use the exposed surface area than the volume of the specimens in determining the rate of corrosion. Erbehtas et al.^[3, 4] used $6.67 \text{ cm}^3/\text{cm}^2$ as the ratio of solution volume (cm^3) to the surface area of the specimens (cm^2). Therefore, as the first objective, the preliminary study in this section examines the influence of the amount of sulfuric acid solution on the change of pH over time.

In addition to the amount of solution, environmental factors were also considered in determining the change of pH. Previous research discussed the immersion of cementitious specimens in chemical sulfuric acid solution but most did not mention whether it was kept in a closed chamber or exposed to atmosphere ^[5-9]. Taking ionic concentration measurements and renewing solutions during the test can expose the test media to the atmosphere ^[4, 10, 11]. The material of the containers used for exposure media also remained a question whether it contributed the change of pH. Therefore, as the second objective, this

paper examined the influence of atmosphere and the materials of the containers (glass and plastic) on the change of pH of the sulfuric acid solution.

Unlike the biological chamber^[12, 13] and benchtop biogenic acidification tests^[4, 14] in which microorganisms are responsible for keeping the pH consistent, chemical acidification test requires the exposure solution to be renewed frequently as the pH of the solution rose over time due to alkalization by the specimens. Since this increase was shown to be higher for solutions with higher pH, more frequent solution refreshments were necessary^[1, 11]. This increased the risk of losing chemical data between old and new solutions such as calcium and sulfate ions concentration. Therefore, as the third objective, this preliminary work examined the effect of using a mixture of sulfuric acid and buffer solution to test the hypothesis that increasing buffer capacity might maintain pH of the solution within the range of ± 0.5 from initial pH.

A.3. Materials and Methods

Type I/II ordinary Portland cement in compliance with ASTM C150/C150M-20^[15] was used to prepare cement paste mixture with water to cement ratio 0.42. Mixing cement paste was performed in a vacuum mixer (Twister Evolution Venturi, Renfert USA, St. Charles, IL) of 1L bowl at 400rpm under 80% vacuum to minimize entrapped air in the mixtures. The mixer is run for two 90-seconds sessions split by approximately 30 seconds to scrape the mixer's wall and blade with a spatula. The fresh paste was then poured into cylindrical molds with 50.8mm in diameter and 101.6mm in height. The cylinders were cured in a moist cabinet at a temperature $23^{\circ}\text{C} \pm 2^{\circ}\text{C}$ and a relative humidity of not less than 98% for 28 days in a sealed condition. After curing, the cylinders were demolded and sliced into disks with thickness $2.65 \pm 0.25\text{mm}$ by using diamond blade wet saw. The middle 60mm portion of the cylinder was used in slicing and the outer 20mm at each end of the cylinder was discarded to avoid defects. The thin-disk specimens were used to immerse in the sulfuric acid solutions at pH2 and pH5 in the tests shown in Table-A1. Only pH2 and pH5 solutions were used in this experiment since they are the lower and upper boundary of the

target range of pH that need to be examined for further research. The pH of each solution was measured by a pH electrode and a benchtop multi-parameter (VWR 89231-586 and VWR Symphony B40PCID, VWR International, Radnor, PA).

Table-A1: Summary of information on the preliminary and exploratory tests

Test No.	No. of Specimens Present in Each Container	Liquid to Specimens Ratio	Tested pH	Objective
1	9	4.2 and 4.67	2, 5	To examine the influence of solution amount that the specimens are immersed.
2	0	-	2, 5	To examine the potential external factors (atmospheric carbonation, material of the container) to affect the pH of the solutions without specimens.
3a	0	-	2, 5	To observe the effect of weak acid mixed with sulfuric acid solution without specimens
3b	9	-	2, 5	To observe the effect of weak acid mixed with sulfuric acid solution with specimens present.

The first test is to examine the effect of solution amount used to immerse cement paste specimens. Two different ratios (4.2 and 4.67) were used to prepare sulfuric acid solution. The ratio of the solution volume to the specimen's volume, 4.2, was used in chemical acid immersion test in House. However, there is argument against using volume to volume ratio since the corrosion is highly induced by the amount of surface area of the specimen. Therefore, some studies suggested to use the ratio of solution volume to the surface area of the specimens' being exposed. In this experiment, the same ratio of 4.2 (volume/volume) used by House is converted to the ratio of solution volume to the specimens' surface area (volume/surface area), 4.67. Two ratios generate two different amounts of solution to be used in immersing the cement paste specimens. Test-1 as described in Table-A1 compared

the consistency of the pHs over time in two different amounts of the same solution. Nine specimens were immersed in each acid solution with pH2 and pH5, both of which are prepared in two different amounts of solutions. The observation lasted for 24 hours.

The second test or Test-2 investigated on potential external contributors of rising pH in sulfuric acid solutions and thus, the cement paste samples were not used. Atmospheric carbonation, and the pH-activated polypropylene containers were investigated as potential factors that may influence the change of pH over 24-hours period. Therefore, in Test-2, sulfuric acid solutions were prepared at pH2 and pH5 and separated into an open glass container, a close glass container, an open plastic container and a close plastic container as shown in Figure-A1. A total of eight cells are created for this test: four for pH2 and another four for pH5. It should be noted that the exposure area to atmosphere is different between open glass and open plastic containers.



Figure-A1: 1). Close glass, 2). Open glass, 3). Open plastic, and 4). Close plastic containers of sulfuric acid solution without any samples.

To resist the neutralization effect of the cement paste specimens, the third test or Test-3 as shown in Table-A1 investigated the buffer capacity of acetate buffer solution, whose buffer capacity is effective roughly within the range of pH2 and pH5 [16, 17]. A buffer solution is made up of a weak acid and its conjugate base or salt. Although integrating its conjugate

salt significantly increases buffer capacity, a weak acid only solution can also provide a mild resistance to pH changes due to external sources. Therefore, Test-3 investigated not only on buffer solutions but also on solutions of only weak acids. Weak acid solutions would be preferred to salted buffer if the former can keep the pH within the desired range for 24 hours as the interference of salt compounds can be ruled out in the reaction system in the cells. Test-3 was divided into two phases: (a) the observation of any pH changes in the sulfuric solutions before any specimens were introduced, and (b) the investigation of buffer capacity in sulfuric acid solutions when specimens were introduced.

A solution of acetic acid and a solution of acetate buffer (a mixture of acetic acid and its salt, sodium acetate) were both prepared at pH5.5, where buffer capacity starts to be effective. Those solutions were separated into two containers and mixed with 98% concentrated sulfuric acid to reduce pH of the two solutions to pH5 and pH2, respectively. Acetic acid solution is more sensitive to changes in pH compared to salted buffer while the latter requires a considerable amount of sulfuric acid to reduce the original pH. As shown in Figure-A2, Test-3a was observed at pH2 and pH5 for 24 hours with 1) a solution of acetic acid, 2) a solution of acetate buffer (a mixture of acetic acid and sodium acetate) and 3) a sulfuric acid solution. Cement paste specimens were introduced into the solutions only after 24 hours when Test-3b was started.

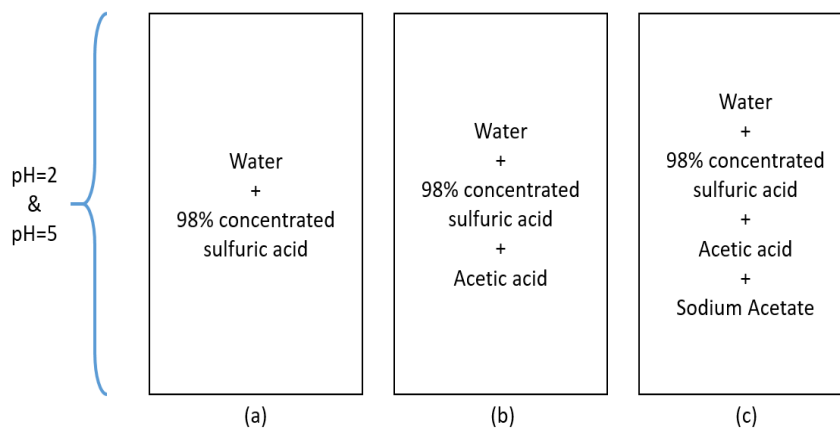


Figure-A2: Three types of solutions in Test-3: a) sulfuric acid solution, b) acetic acid solution with sulfuric acid, and c) acetate buffer solution with sulfuric acid

A.4. Results and Discussion

Test-1 observed the rapid rise of pH in sulfuric acid solutions when cement paste specimens were immersed. As shown in Figure-A3, pH2 solution rose to pH2.95, pH5 solution to pH9.37 within half an hour for solution to specimen ratio 4.2. The rate of change of pH in both containers were so fast that it was not practical to run an actual acid immersion experiment as the solutions would be required to refresh approximately every 30 minutes. In the container with solution to specimen ratio of 4.67, pH5 solution also jumped to about pH10 although the consistency in pH2 solution improved. Therefore, the effect of increasing solution volume can be seen in pH2 and not in pH5.

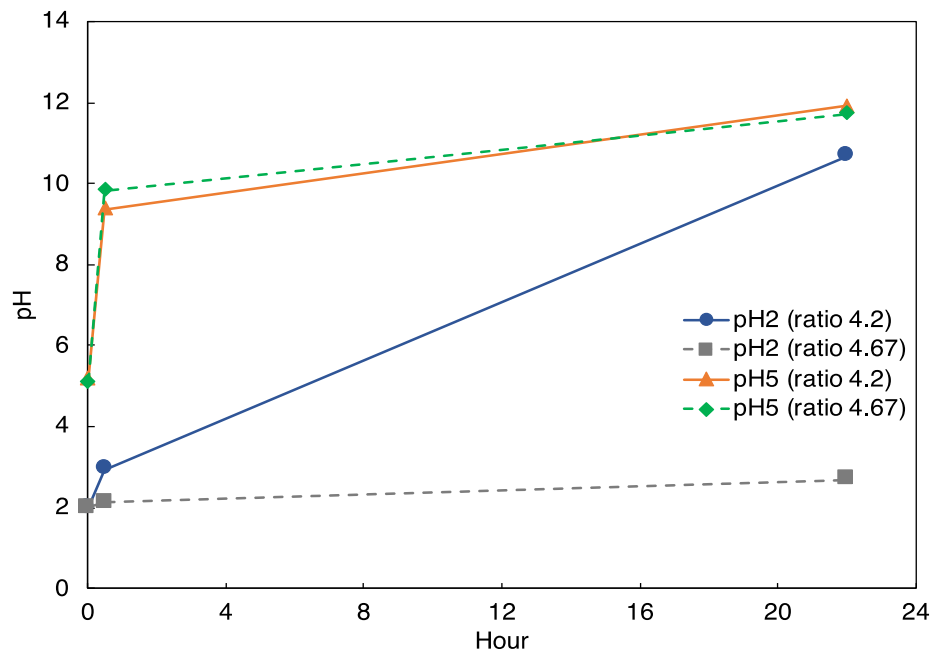


Figure-A3: pH5 rose significantly in the first 30 minutes in both ratios while pH2 only slightly increased in the larger amount of solution.

To investigate any potential factors except the cause of cement paste specimens that may have affected the change of pH, a more comprehensive test was conducted without specimens in Test-2. The pH is stable in pH2 solutions in different containers while the pHs in pH5 containers generally rose 1.5 and 2 units of pH. Plastic containers increased the pH more than glass counterparts especially when the container was open and exposed

to atmosphere. Open glass container has a slightly higher pH than close glass container. Therefore, in addition to cement paste samples, it should be noted that the material of the container and atmospheric exposure also have impacts on pH of their corresponding solutions when the starting pH is high.

All pH2 solutions remained consistent over time whether the cell is close or open and glass or plastic. Figure-A4 showed the ability of pH2 solution that can keep the pH stable from external disturbances. On the contrary, pH5 solutions encountered a rise although it was lower than solutions exposed to cement paste samples. Figure-A5 showed that the pH in plastic containers tended to increase higher than in glass containers. And the data in plastic containers showed that atmospheric exposure had a relative impact in stimulating pH although it was not significant in glass containers. Although the solutions were planned to be kept in close plastic containers in the actual experiment, it should be noted that the cells were exposed to atmosphere when measurements were taken.

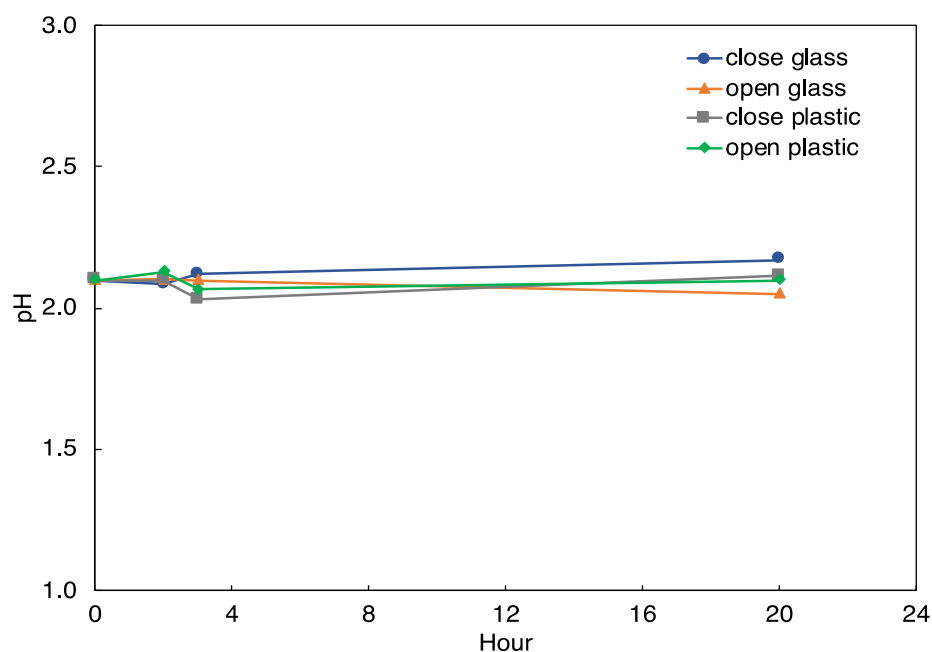


Figure-A4: pH2 solution had capacity to prevent external pH stimulations.

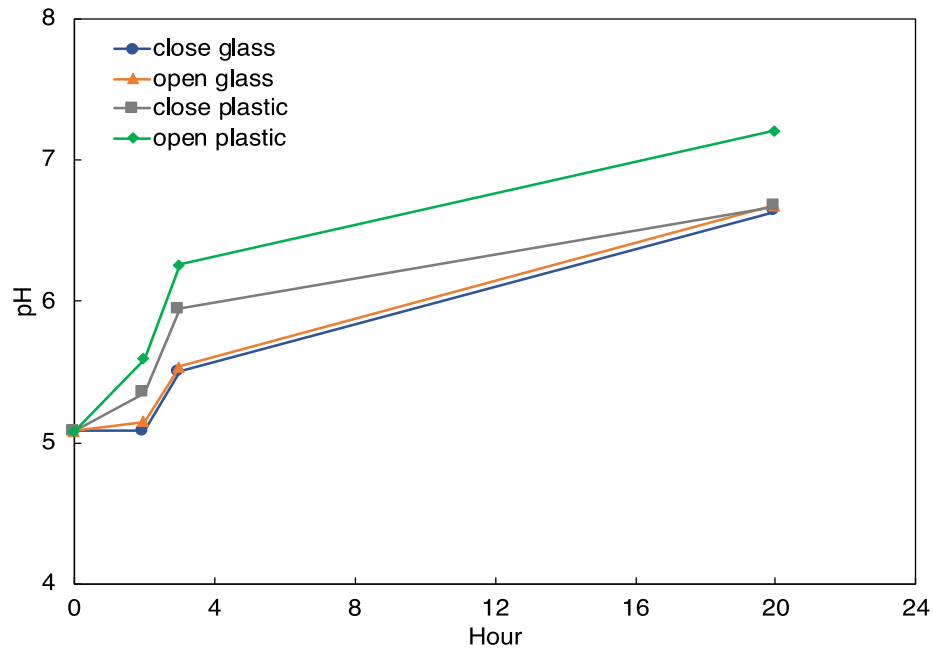


Figure-A5: pH5 solution encountered external pH stimulations. Atmosphere and plastic container relatively affected the change of pH.

Since sulfuric acid solution of pH5 were neutralized quickly due to calcium leaching of cement paste samples and other external factors such as atmospheric carbonation, and slight pH-activation of plastic containers, buffer solution was introduced into sulfuric acid solution to provide buffer capacity in Test-3. However, it should be noted that inclusion of salt in buffer solutions can interfere the default reaction system that takes place in cement paste specimens exposed to only sulfuric acid solution.

In Test-3a, all three solutions in pH2 containers and the two buffers in pH5 solutions remained stable except the sulfuric acid solution in pH-5 cell without any buffer jumped to pH6.25 as expected. The ability of buffer solutions that can keep their pH consistent shows that the disturbances of atmospheric carbonation, potential pH-activation of plastic containers, or other external factors that have not been detected can be ruled out in contributing the rise of pH when no specimens are present.

If the solutions with only weak acids can keep the pH consistent in 24 hours, these solutions could be a suitable candidate to be used in actual chemical sulfuric acid immersion test without concern for potential interference of the salt, source of sodium ions, in the reaction system. However, the results in both Figure-A6 and Figure-A7 showed that when cement paste samples were introduced into the solutions, acetic acid-only solutions could not keep the pH consistent and even acetate buffer encounters a relative increase in pH within 24 hours in both pH2 and pH5. Therefore, the use of high pH solutions (the lower pHs in stage-2 corrosion) in chemical sulfuric acid immersion test is not practical without constant adjustment of pH or automated titration in the solutions.

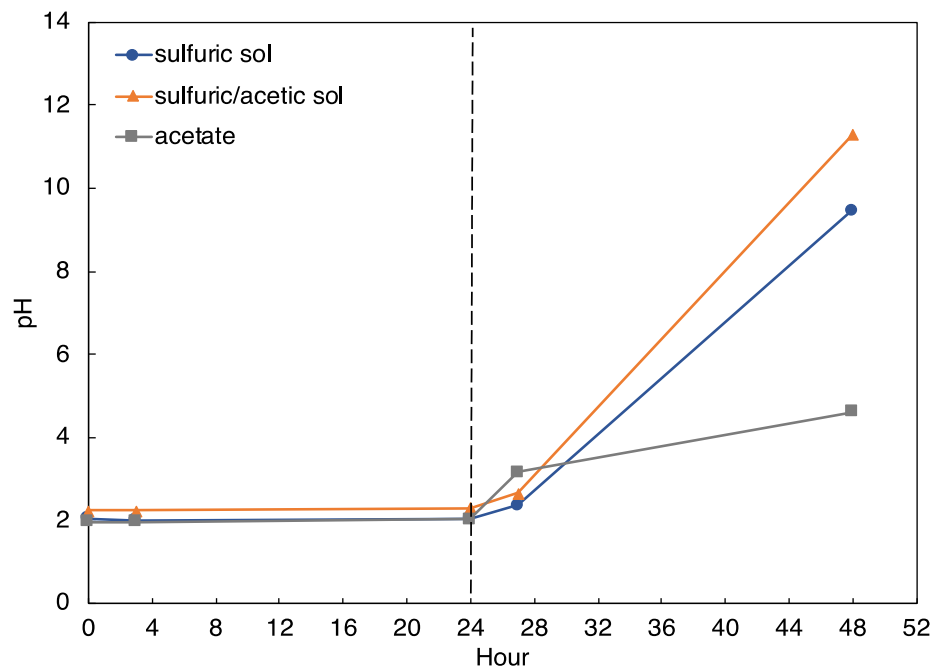


Figure-A6: even acetate buffer solution in pH2 encountered the rise of pH due to one cement paste specimen

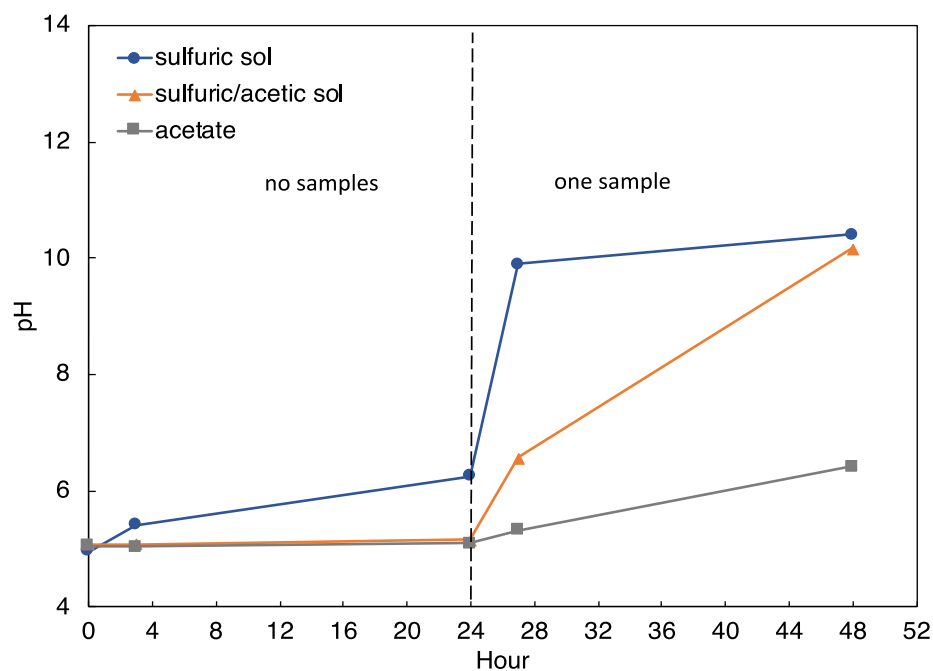


Figure-A7: rapid rise of pH occurred in sulfuric acid solution and gradual rise of pH in buffer solutions.

A.5. Conclusion

The pH2 solution was influenced by the amount of solution but pH5 solution has no significant effect. The pH became more consistent despite a slight upward trend in pH2 solution when the amount of solution increased. The pH trends almost overlapped each other in pH5 solutions regardless of the volume. Therefore, the amount of solution alone was not sufficient to maintain the pH for solutions in higher pHs.

External conditions have little effect on pH2 solutions. However, exposure to atmosphere and the plastic container affected the pH in the solution initially at pH5. Atmospheric exposure increased the pH from pH5 to pH 6.67 in glass container and to pH 7.20 in plastic container. The solution in plastic containers encountered higher pH rise than the solution in glass containers.

Adding a weak acid in both sulfuric acid pH2 and pH5 solutions could not keep the pH consistent over time. Once a paste specimen was submerged, the pH in both pH2 and pH5 solutions rose significantly. A mixture of buffer solution in addition to weak acid slowed the upward movement but it was not sufficient to keep the pH in the range of ± 0.5 from initial pH. The solution with initial pH2 rose to pH4.61 and the solution with initial pH5 increased to pH6.42. Therefore, it was observed that sulfuric acid solutions with buffer capacity only reduced alkalization but not sufficiently kept the pH consistent.

These preliminary and exploratory studies examined the factors that affected the change of pH in sulfuric acid solutions so that the pH can be kept consistent over time in higher pH solutions by identifying and resolving the possible issues. The amount of solution relatively slowed down pH2 solution but had no effect on pH5 solution. Atmospheric exposure that would be encountered during measurements of ionic concentration and the plastic container also contributed in raising pHs. Even the solutions with buffer capacity were not successful in maintaining pH when cementitious specimens were immersed. These observations led the authors to experiment an automatically titrated chemical acidification test in which the pH of the test media remained consistent over time by dosing concentrated sulfuric acid accordingly.

A.6. References

1. House, M., et al., *Concrete Resistance to Sulfuric Acid Immersion: The Influence of Testing Details and Mixture Design on Performance as It Relates to Microbially Induced Corrosion*. *Advances in Civil Engineering Materials*, 2019. **8**(1): p. 544-557.
2. *Standard Test Methods for Determining the Chemical Resistance of Concrete Products to Acid Attack*. 2020, ASTM C1898: ASTM International, West Conshohocken, PA.
3. Erbektas, A.R., O.B. Isgor, and W.J. Weiss, *Comparison of Chemical and Biogenic Acid Attack on Concrete*. *ACI Materials Journal*, 2020. **117**(1): p. 9.
4. Erbektas, A.R., O.B. Isgor, and W.J. Weiss, *An accelerated testing protocol for assessing microbially induced concrete deterioration during the bacterial attachment phase*. *Cement and Concrete Composites*, 2019. **104**: p. 103339.
5. Fattuhi, N.I. and B.P. Hughes, *SRPC and modified concretes subjected to severe sulphuric acid attack*. *Magazine of Concrete Research*, 1988. **40**(144): p. 159-166.
6. Fattuhi, N.I. and B.P. Hughes, *The performance of cement paste and concrete subjected to sulphuric acid attack*. *Cement and Concrete Research*, 1988. **18**(4): p. 545-553.
7. Hewayde, E., E.N. Allouche, and G.F. Nakhla, *Experimental Investigations of the Effect of Selected Admixtures on the Resistance of Concrete to Sulfuric Acid Attack*, in *New Pipeline Technologies, Security, and Safety*. 2003. p. 504-513.
8. Hewayde, E., et al., *Effect of Mixture Design Parameters and Wetting-Drying Cycles on Resistance of Concrete to Sulfuric Acid Attack*. *Journal of Materials in Civil Engineering*, 2007. **19**(2): p. 155-163.
9. Hewayde, E., et al., *Using concrete admixtures for sulphuric acid resistance*. *Proceedings of the Institution of Civil Engineers - Construction Materials*, 2007. **160**(1): p. 25-35.

10. De Belie, N., et al., *Experimental research and prediction of the effect of chemical and biogenic sulfuric acid on different types of commercially produced concrete sewer pipes*. Cement and Concrete Research, 2004. **34**(12): p. 2223-2236.
11. Erbektas, A.R., O. Isgor, and W. Weiss, *Comparison of Chemical and Biogenic Acid Attack on Concrete*. ACI Materials Journal, 2020. **117**.
12. House, M. *Using biological and physico-chemical test methods to assess the role of concrete mixture design in resistance to microbially induced corrosion*. 2013.
13. Sand, W., E. Bock, and D. White. *Biotest system for rapid evaluation of concrete resistance to sulfur-oxidizing bacteria*. 1987.
14. *Standard Test Methods for Determination of the Effects of Biogenic Acidification on Concrete Antimicrobial Additives and/or Concrete Products*. 2020, ASTM C1904-20: ASTM International, West Conshohocken, PA.
15. *Standard Specification for Portland Cement*. 2020, ASTM C150/C150M-20: ASTM International, West Conshohocken, PA.
16. Stoll, V.S., V.S. Stoll, and J.S. Blanchard, *Buffers: principles and practice*. Methods in enzymology, 2009. **463**: p. 43-56.
17. Dempsey, B. and D.D. Perrin, *Buffers for pH and metal ion control*, ed. B. Dempsey. 1974, London, New York: London, Chapman and Hall
New York, Wiley.